Maria Inês Gonçalves Lobato de Almeida

Bachelor of Science in Biomedical Engineering

Inertial sensor based full body 3D kinematics in the differential diagnosis between Parkinson's Disease and mimics

Dissertation submitted for the Master Degree in Biomedical Engineering

Advisers: Dr Ricardo Matias, PhD, Champalimaud Foundation.

Prof. Dr ª Carla Quintão, Auxiliary Professor, Faculty of Sciences and Technologies, New University of Lisbon.

Examination Committee:

Chairperson: Prof. Dr José Luís Constantino Ferreira

Adviser: Prof. Dr ª Carla Maria Quintão Pereira

Examiner: Prof. Dr ª Cláudia Regina Pereira Quaresma

FACULDADE DE CIÊNCIAS E TECNOLOGIA
UNIVERSIDADE NOVA DE LISBOA

September, 2019

Inertial sensor based full body 3D kinematics in the differential diagnosis between Parkinson's Disease and mimics

"With the new day comes new strength and new thought."

Eleanor Roosevelt

Acknowledgements

It is with great pleasure and satisfaction that I finish this important step of my life. This work would not be possible without the help, care and support of some people who helped me to fulfil my goals, to whom I could not fail to express my sincere thanks.

First, I would like to express my gratitude to Professor Albino Oliveira-Maia for the opportunity for the concretization of this thesis. Thank you for the opportunity to have worked in such a fascinating project.

To Dr. Francisco Oliveira, a sincerely thanks for all the advices and support.

I also would like to thank to Professor Carla Quintão for being so friendly and kind and, for all the support during these five years.

An indescribable thanks to Ana Castro Verde and Mónica Mendonça Silva for their long conversations, for sharing my fears and accomplishments, for their attention and support, but above all for their friendship during these months. I also would like to thank to my college friends, especially to Kate, Juju, Patrícia fan, Krupii, Jo, and Di with whom I shared moments of true happiness, joy, but also despair during these five years.

Last but not least, I would like to thank to my family, especially my mummy and siblings, for their everyday support, care and encouragement. Thank you for being my inspiration and for valuing the importance of this document. But a special thanks to my granny Silvina without whom I would not have achieved what I have got today.

Thank you very much to all of you!

Abstract

The differential diagnosis of Parkinson's Disease (PD) remains challenging with frequent mis and underdiagnosis. DAT-Scan has been a useful technique for assessing the lost integrity of the nigrostriatal pathway in PD and differentiating true parkinsonism from mimics. However, DAT-Scan remains unavailable in most non-specialized clinical centres, making imperative the search for other easy and low-cost solutions. This dissertation aimed to investigate the role of inertial sensors in distinguishing between the denervated and the non-denervated individuals.

In this dissertation, we've used Inertial Sensor Based 3D Full Body Kinematics (FBK) and tested if this technique was able to distinguish between patients with changes in the DAT-Scan from those without. This was divided into two parts, being that firstly, a group of individuals was referred by the attending physician for DAT-Scan (^{123}I-FP-CIT SPECT) to be able to compare FBK in those with and without evidence of dopaminergic depletion. Second, it was tested whether FBK could be used as a metric for the severity of dopaminergic depletion.

Twenty-one patients participated in this study, being recruited from the Nuclear Medicine Unit in the Champalimaud Clinical Centre (CCC), Lisbon. Within these 21 patients, 10 of them had denervation (mean age, 68.4 ± 7.8 years) and the remaining 11 (mean age, 66.6 ± 7.4 years) did not present denervation.

The analysis between the worst uptake ratio features and dimensional features, as well as the asymmetry indexes in the striatum revealed significant differences between denervated and non-denervated individuals. On the contrary, the kinematics did not do it. Overall, based on the collected kinematics data, it was identified that there was not any significant correlation between the kinematics and the DAT-Scan. What means that these kinematics variables were not able to explain the DAT-Scan. On the other hand, it was also checked that the kinematics data were strongly correlated to the motor symptoms (MDS-UPDRS III).

This way, it was concluded that the classical biomechanics did not distinguish denervated from non-denervated individuals. Therefore, the kinematics could not give the same answer as the DAT-Scan. In spite of these results it would be relevant to keep researching other methods in order to find out the distinction between the denervation and no denervation in a low-cost way.

Keywords: Parkinson's Disease, DAT-Scan, Inertial Sensors, Motion Capture System, Kinematics.

Resumo

O diagnóstico diferencial da doença de Parkinson (DP) permanece desafiador com frequentes erros de diagnóstico e subdiagnóstico. O DAT-Scan tem sido uma técnica útil para avaliar a perda da integridade da via nigrostriatal na DP e diferenciar o parkinsonismo verdadeiro das outras síndromes parkinsonianas. No entanto, o DAT-Scan permanece indisponível na maioria dos centros clínicos não especializados, o que torna imperativa a busca por outras soluções fáceis e de baixo custo. Esta dissertação teve como objetivo investigar o papel dos sensores inerciais a distinção entre indivíduos desnervados e não desnervados.

Nesta dissertação, usámos a cinemática de corpo inteiro (FBK) 3D baseada em sensores inerciais e testámos se essa técnica era capaz de distinguir entre pacientes com alterações no DAT-Scan daqueles sem. Esta foi dividida em duas partes. em primeiro lugar, um grupo de indivíduos foi encaminhado pelo médico assistente para o DAT-Scan (^{123}I-FP-CIT SPECT) para poder comparar a FBK naqueles com e sem evidência de depleção dopaminérgica. Segundo, foi testado se a FBK poderia ser usada como uma métrica para a severidade da depleção dopaminérgica.

O estudo incluiu 21 pacientes da Unidade de Medicina Nuclear do Centro Clínico Champalimaud (CCC), em Lisboa. Desses 21 pacientes, 10 deles apresentaram desnervação (idade média de 68,4 ± 7,8 anos) e os restantes 11 (idade média de 66,6 ± 7,4 anos) não apresentaram desnervação.

A análise das piores taxas de absorção e das características dimensionais no estriado, assim como os índices de assimetria revelaram diferenças significativas entre os indivíduos desnervados e não desnervados. Pelo contrário, a cinemática não. No geral, com base nos dados cinemáticos recolhidos, verificou-se que não havia uma correlação significativa entre a cinemática e o DAT-Scan. O que significa que as variáveis cinemáticas usadas não podem explicar o DAT-Scan. Por outro lado, os dados também mostraram que a cinemática está fortemente correlacionada com os sintomas motores (MDS-UPDRS III).

Assim, concluiu-se que a biomecânica clássica não distingue os indivíduos desnervados dos não desnervados. Pelo que, a cinemática não pode dar a mesma resposta que o DAT-Scan. Apesar destes resultados, será relevante continuar a investigar outros métodos para distinguir entre denervação e não-denervação de uma maneira económica.

Palavras-chave: Doença de Parkinson, DAT-Scan, Sensores Inerciais, Sistema de Captura de Movimento, Cinemática.

Table of Contents

List of Figures

List of Tables

Acronyms and Abbreviations

^{123}I-FP-CIT SPECT	DAT-Scan
3D	Three-Dimensional
AC	Alternating Current
APS	Atypical Parkinsonian Syndromes
BG	Basal Ganglia
CBD	Corticobasal Degeneration
CBP	Caudate Binding Potential
CCC	Champalimaud Clinical Centre
DA	Dopamine
DAT	Dopamine Transporter
DC	Direct Current
DIP	Drug-Induced Parkinsonism
DIVs	Distribution Volume Ratios
DLB	Dementia with Lewy Body
ET	Essential Tremor
FBK	Full Body Kinematics
IK	Inverse Kinematics
IMUs	Inertial Measurement Units
MDS-UPDRS	Movement Disorder Society-Unified Parkinson's Disease Rating Scale
MS	Motor Symptoms
MSA	Multiple System Atrophy
NMS	Non-Motor Symptoms
PBP	Putamen Binding Potential
PCR	Putamen to Caudate Ratio
PD	Parkinson’s Disease
PET	Positron Emission Tomography
PS	Parkinsonian Syndrome
PSP	Progressive Supranuclear Palsy
ROI	Region of Interest
SBP	Striatum Binding Potential
SBR	Specific Binding Ratio
SN	Substantia Nigra
SNpc	Substantia Nigra Pars Compacta
SPECT	Single Photon Emission Computed Tomography
UPDRS	Unified Parkinson's Disease Rating Scale
VP	Vascular Parkinsonism

1 Introduction

1.1 Motivation

The nervous system plays an important role in the human body once it affects the sensory and motor functions. Therefore, the research on the neural development is of great importance to improve understanding of the brain functions and the human illnesses. Any disturbance on the neuronal connectivity can lead to brain dysfunction and diseases, such as idiopathic Parkinson's disease (PD) [1] that is one of the forms of Parkinsonism. Parkinsonism is a term that covers several conditions such as PD and other neurological conditions with similar symptoms for example: slowness of voluntary movements (bradykinesia), rigidity and problems with walking [2]. Parkinson's disease is a neurodegenerative brain disorder where some nerve cells break down slowly or die. The symptoms include an ongoing damage of motor control, once they are due to a loss of the neurons that produce a chemical messenger in the brain called dopamine (DA). When its levels decrease it causes the abnormal brain activity, leading to the symptoms of PD. These symptoms can take years to develop and most people live for many years with the disease [3].

Currently, the prevalence of PD includes 180 cases per 100 thousand inhabitants in people over 50 years in Portugal [4]. It is estimated that the number of people with this disease will increase in the coming decades worldwide [5], [6].

The Parkinson's disease is usually diagnosed clinically by the presence of parkinsonism, i.e., bradykinesia plus some other motor symptoms (MS). However, when the MS appears clinically, there has already been a 50% reduction in the dopaminergic nigrostriatal cells [7]. Today the most common used method to exclude the PD is the DAT-Scan, allowing to observe the integrity of the dopamine transporters (DATs). The DAT-Scan is a medical examination that can not only provide the information for the patients suspected of having a dopaminergic deficiency but it can also discriminate the parkinsonian syndromes (PSs). Still, this method is very expensive, slow, and mostly analyzed by the qualitative and the subjective ratings obtained by the human interpretation of the presentation of the disease signs and the symptoms at the clinical visits [8].

In recent years, gait analysis has demonstrated effectiveness in pre-treatment evaluation, surgical decision making, postoperative follow-up, and management of patients. It is known that human locomotion involves the integration of intricate sensory information within the nervous system, resulting in motor commands to control muscle contraction and subsequent joint movement [9], [10].

The quantitative, objective, and easy wearable sensors (e.g. inertial sensors) have been also developed for quantifying PD signs. They are smart electronic devices with microcontrollers that can be incorporated into clothing or worn in the body as implants or accessories which enable to exchange data, without requiring human intervention. These devices have the potential to improve significantly both clinical diagnosis and management in PD and the conduct of clinical studies. This technology allows relevant measurements through a cheap, reliable and validated disease process [11].

In this context, it is relevant to apply kinematic models in the inertial sensors to make an assessment as far as concerned the balance and the gait abnormalities in the early stages of the PD. As a motivation, it is expected that the inertial sensors can answer at the same mode as the DAT-Scan because it is an inexpensive and quick method.

1.2 Objectives and Dissertation Structure

The main goal of this work is to distinguish between individuals with and without denervation, whose diagnosis is unknown, as defined by the DAT-Scan result, through the use of full body kinematics (FBK). The secondary objective is to determine if there is a kinematics relationship with the dopaminergic system.

The dissertation is structured as presented as follows:

- Chapter 1 describes the motivation of the study, the aim and objectives of the research.

- Chapter 2 provides a brief introduction to Parkinson's disease and related problems. The reader will be presented with an explanation about the technique, properties and utility of DAT-Scan. The role of DAT-Scan in the diagnosis of Parkinson's and the problem of the use of DAT-Scan. It also describes the concepts related to gait assessment, kinematics and inertial sensors.

- In chapter 3, the materials and methods used for the kinematics analysis and for the imaging processing are presented.

- Chapter 4 contains the results of this study.
- Chapter 5 indicates the overall discussion and the limitations from this dissertation work.
- Finally, chapter 6 presents the conclusions and future perspectives which summarize the dissertation's findings and it suggests the next steps of this study.

2 Literature Review

This chapter provides a brief introduction about Parkinson's disease. It provides some notion about the concepts of ^{123}I-FP-CIT SPECT, gait analysis, kinematics and motion caption with inertial sensors.

2.1 Parkinson's Disease

The Parkinson's disease (PD) is a slow, progressive and neurodegenerative disorder, with no cure currently. The PD is characterized by the neural degeneration in the specific brain regions, such as the dopaminergic neurons of the substantia nigra pars compacta (SNpc). That means it occurs the progressive loss of the dopaminergic neurons within the SNpc and their axon terminals in the striatum [12].

The substantia nigra (SN), which is placed in the midbrain, constitutes a part of the basal ganglia (BG) that is a highly organized network, where the different regions of the brain are activated. That one coordinates multiple aspects of the cognition, such as: controlling movement through their connections with the motor cortex and providing associative learning, planning, working memory, and emotion. The main components of the BG are in the striatum. This last one is constituted by the caudate nucleus and the putamen. The caudate nucleus is one of the structures that makes up the corpus striatum, and the putamen is a round structure located at the base of the forebrain [13].

SNpc sends messages to the striatum via neurons that are rich in the neurotransmitter dopamine (DA), forming the nigrostriatal pathway, which helps to stimulate the cerebral cortex and initiate movement. In **Figure 2.1** is shown how it is passed the information via neurons. The information is conveyed through two kinds of neurons: the *presynaptic* and the *postsynaptic* ones.

The *presynaptic neurons* are constituted by *store vesicles,* where DA is stored and, subsequently, released through the *dopamine transporters* (DAT). DAT is a sodium chloride dependent protein in dopaminergic terminals and it is responsible for the reuptake of *dopamine* from the synaptic cleft back to the *presynaptic neurons* at the moment of information transmission. This DA is not all lost because it is captured in the *presynaptic neurons* by the *DAT and re-storage,* after being released by *dopamine receptors* of *postsynaptic neurons* [14],[15].

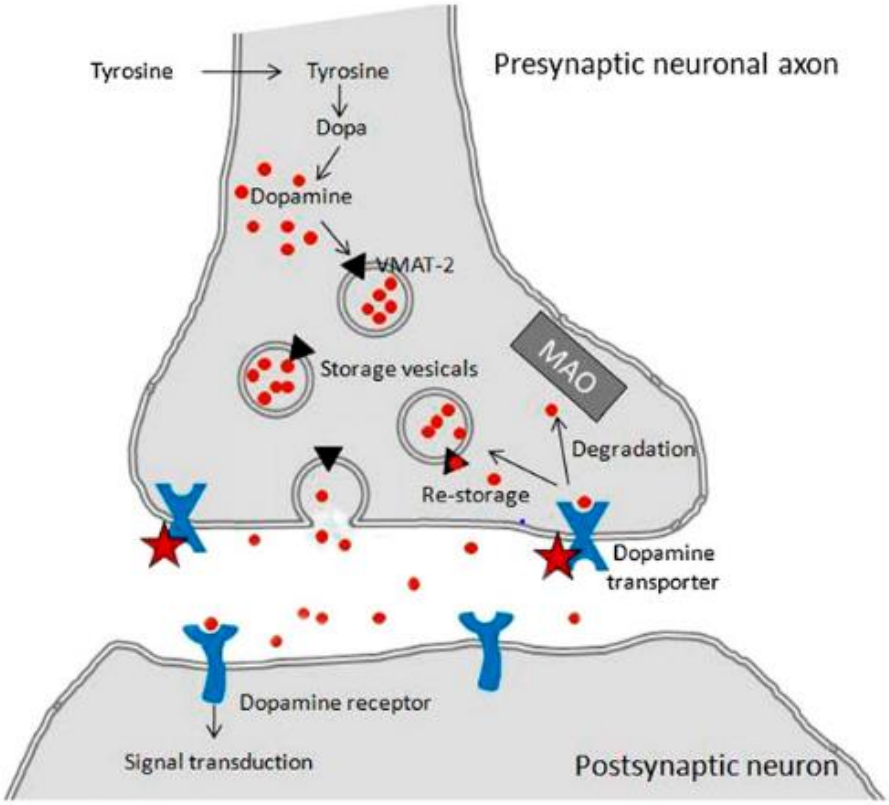

Figure 2.1 | Schematic representation of dopaminergic neurotransmitter system [14].

2.1.1 Characteristics of the Parkinson's Disease

The cause of PD is usually unknown (idiopathic). However, the lifestyle, the environmental and the genetic factors are considered etiological determinants. Moreover, the advanced age is another significant risk factor [16]. It is generally considered that known genetic causes may be relevant in more than 5% of the total PD population, but some propose that monogenetic causes may be involved in as many as 5–10% of the PD population [5].

The clinical diagnosis of classic PD is based on identifying clinical characteristics related to striatal dopamine depletion that typically manifest as motor signs and symptoms (MS) - *bradykinesia, tremor, rigidity, and postural instability* - which are accompanied or often even preceded by non-motor symptoms (NMS) [16]. These MS just appear after a 50-70% reduction of striatal dopamine which corresponds to 50% cell death of dopaminergic neurons of the SNpc. Patients with PD present first with unilateral symptoms but gradually it can progress involving both sides [17]. However, these ones may not all be present.

The symptoms referred above are going to be described:

Bradykinesia is also known as a slowness of movement and it is the most common symptom of PD, because it is necessary for the diagnosis. It is responsible for inducing difficulties with rapid repeated movements [18]. Beyond the slowness in performing activities of daily living, the slow movement and the reaction times, *bradykinesia* presents other manifestations like the loss of spontaneous movements and gesturing, loss of facial expression, decreased blinking and reduced arm swing while walking [19].

A tremor is an involuntary trembling movement or shake. Characteristically occurring at rest, the classic slow, rhythmic tremor of Parkinson's disease typically starts in one hand, foot, or leg and can eventually affect both sides of the body. The tremor that occurs in Parkinson's disease is different from almost all other tremors because it is a "resting tremor", present primarily at rest. It goes away with movement but often returns when the limb is held in one position, as in holding a spoon or fork to the mouth, which is why those with Parkinson's are known to spill things. Parkinson's disease tremor may affect almost any part of the body, but most commonly involves the fingers, followed next most commonly by the hands, jaw, and feet [20]. It occurs when a body part is totally supported at rest and tends to stop when an intended action is carried out. It can affect the hands, legs, lips, and tongue [19].

Rigidity occurs when there are series of catches or stalls as a person's arms or legs are passively moved by someone else. It is characterized by increased resistance, once the muscles become rigid because of their inability to relax. It may occur both at the proximal level, for example in the neck, shoulders, and hips, as well as at the distal level, such as the wrists and ankles [21]. The *rigidity* can limit muscles from stretching and relaxing as they should. It can manifest at the level of rigid muscles through reduced facial expression, difficulty turning when walking, in bed and getting out of a chair or bed, reduced arm swing when walking and difficulty with everyday activities such as dressing, cutting food and writing, for example [20].

Finally, *postural instability* is due to the loss of postural reflexes, which are usually a manifestation of the late stages of PD that may occur after the appearance of other clinical features. It causes problems with balance and can lead to falls. Other parkinsonian symptoms, orthostatic hypotension, age related sensory changes and the ability to integrate visual sensory input are several features that influence the occurrence of *postural instability* [19].

As mentioned above there are also NMS of PD including behavioral and psychiatric problems such as: dementia, psychosis, cognitive impairment, addiction and compulsion, depression and anxiety, fatigue, gastrointestinal and olfactory dysfunction. Yet, there are other neurodegenerative diseases when these clinical features appear, which means that it is hard to diagnose PD [22].

2.1.2 Differential Diagnosis Problem of Parkinson's Disease

The different causes of parkinsonism can be classified into two distinct groups: diseases with nigrostriatal cell loss such as Parkinson's disease (PD), Progressive Supranuclear Palsy (PSP), Multiple System Atrophy (MSA), Corticobasal Degeneration (CBD), and Dementia with Lewy body (DLB) and diseases without nigrostriatal cell loss such as Drug-Induced Parkinsonism (DIP), Essential Tremor (ET), Vascular Parkinsonism (VP) [8].

Progressive Supranuclear Palsy is sometimes misdiagnosed as Parkinson's disease because of the similarity to some symptoms during the early stages of the disease, such as: rigidity, bradykinesia, and movement difficulties. However, PSP progresses much faster, causes more severe symptoms, and it has a significantly reduced life expectancy. There are notable differences in people with PSP, for instance: people find it hard to look up or down, whereas people with PD may experience other eye-related problems, including double vision, uncontrolled blinking or excessive watering; it concerns posture, people with PSP tend to stand straight or tilt their heads backward, while people with PD usually bend forwards; the tremor that is almost universal in people with PD is rare in PSP, etc. [23].

Multiple System Atrophy is often mistaken for Parkinson as it tends initially to present similarities because it presents problems, particularly related to movement, balance and other autonomic body functions. Besides that, MSA progresses faster. According to some studies the degree of loss was higher in putamen than caudate in both PD and MSA patients. However, MSA patients showed a more symmetric loss of striatal DAT in both caudate and putamen than PD patients and MSA patients had significantly increased distribution volume ratios (DVRs) in the posterior putamen compared with PD patients [24].

Dementia with Lewy bodies are the pathological hallmark of Parkinson's disease. Both DLB and PD are characterized pathologically by the presence of Lewy bodies (abnormal aggregates of protein that develop inside nerve cells), though in PD patients there is greater neuronal loss within the SN whereas in DLB patients there is greater cortical β-amyloid[1] deposition. In PD they appear in the SN in the midbrain, while in DLB they are more widely distributed throughout the cerebral cortex. People with DLB may have stiff muscles, slow movement and tremor like someone with PD [16].

Other diseases, for example, DIP, ET, or vascular parkinsonism (VP) also share common features with PD [25].

Drug-Induced Parkinsonism is developed when patients are treated with neuroleptic or dopamine receptor blocking agents. The differentiation between PD and DIP is difficult to assess in clinical grounds alone.

[1] **β-amyloid** are protein fragments that are toxic to neurons and their synapses [16].

Essential Tremor is a slow common condition that results in trembling in the hands or arms, which in some cases can subsequently spread to cause tremor of the head, legs, trunk or voice [26]. It is quite often confused with Parkinson's disease since people with Parkinson also experience tremors, but in PD the trembling is usually more apparent when the hands are resting on the affected person's lap or when walking. It also appears first in ET shaking in both hands but tremor usually starts in one side of the body in PD, typically beginning in a hand, and then it spreads to the rest of the body. There are also other signs in PD that are not seen in ET, for instance: rigidity, bradykinesia or gait disturbance. Sometimes, it is difficult to distinguish between PD and ET and misdiagnoses have been made [27], [28].

A possible diagnosis of PD may be confirmed by the appearance of MS associated with the degeneration of nigrostriatal dopaminergic neurons or if the person responds positively to medication for Parkinson. This is different from what happens with atypical parkinsonian syndromes (APSs) (e.g., PSP, MSA, CBD, and DBL) that are characterized by poor response to antiparkinsonian medication and rapid clinical deterioration, which are often confused with PD [29].

Thus, the differential diagnosis of PD is extensive. There is no definite test to confirm the cause of parkinsonism in clinical practice. Misdiagnoses can occur because symptoms vary from person to person and there is a number of other diseases that have similar symptoms [30].

2.1.3 Monitoring the Progression of the Parkinson's Disease

The rate of progression of dopaminergic degeneration is much faster in PD than in normal aging. Pathologic studies investigating the rate of PD progression have been limited to patients with severe illness of long duration and rely entirely on cross-sectional data. The stage and severity of PD is an important factor to consider for taking effective therapeutic decisions [25].

There are many scales to evaluate impairment disability of motor impairment, as well as to monitor disease progression in patients with PD. Among these, the most well-established scale is the Unified Parkinson's Disease Rating Scale (UPDRS). The Movement Disorder Society-Unified Parkinson's Disease Rating Scale (MDS-UPDRS) is the updated and revised version of the original UPDRS with new items devoted non-motor elements of PD. It provides a comprehensive assessment of the clinical features, both motor as well as non-motor, and it is a flexible tool to monitor the course of PD and the degree of disability. This last one, it will be used in this study but only be considering the part referent to the motor function. The progression of PD usually starts from unilateral (Stage 1), to bilateral without balance difficulties (Stage 2), followed by the presence of postural instability (Stage

3), to loss of physical independence (Stage 4), and being wheel-chair or bed-bound unless aided (Stage 5). The MDS-UPDRS scale allows to categorize PD as early stage (Stage 1 and 2), moderate stage (Stage 3) and late stage (Stage 4 and 5). This scale consists of four parts. Part I assesses the non-motor experiences of daily living, i.e., evaluate mental activity, behaviour, and mood. Part II regards to motor activities of daily living such as: speech, swallowing, handwriting, dressing, hygiene, falling, salivating, turning in bed, walking, and cutting food. Part III is motor examination, which means that it evaluates the motor function. Part IV assesses motor complications such as dyskinesias and motor fluctuations which are strongly related to the duration of disease, and the duration of levodopa treatment [31].

Longitudinal studies show that UPDRS scores increase over time, which may be crucial to clinical decision making, particularly in need to introduce symptomatic therapy. It is also known from these studies that the MDS-UPDRS scale is strongly correlated with the original UPDRS and the other disability measures, quality of life scales and disease duration, what makes the former be more sensitive to changes in PD than the original one. Therefore, the MDS-UPDRS provides a wide spectrum of assessments and it is a reliable and sensitive instrument for estimating the progression and severity in PD [32].

2.2 ^{123}I-FP-CIT SPECT

2.2.1 Technique and Properties

Imaging of the DAT with ^{123}I-FP-CIT (commercially available as DAT-Scan™) and single-photon emission computed tomography (SPECT) is the most widely used nuclear medicine technique for routine confirmation of dopaminergic degeneration during the assessment of patients with suspected degenerative parkinsonism [33].

This test consists of two steps: Firstly, it is given an ^{123}I-Ioflupane injection, radioactive decay of ^{123}I-Ioflupane emits γ radiation, that tags the dopamine transporters. The main metabolic product of ^{123}I-Ioflupane is FP-CIT acid, a polar compound that is unable to cross the blood-brain barrier [34]. Secondly, it involves a γ camera (**Figure 2.2**) [35], which records the iodine radioactivity of several DAT-rich subregions of the brain through images showing the location and density of dopamine cells [36].

Thus, the ^{123}I-FP-CIT SPECT shows how blood flows to tissues and organs, and it allows for detecting the loss of dopaminergic neurons.

Figure 2.2 | Example of DAT-Scan device [35].

DAT-Scan is available only with a medical prescription and it is indicated for adult patients who have parkinsonian syndrome (PS) symptoms. The radioactive exposure and risk associated are somewhat small (the amount of radiation as similar to regular x-rays). Forty-eight hours post-injection, about 60% of the injected radioactivity is excreted in the urine about 14% in fecal excretion. Potential side effects include headache, nausea, stomach upset, dry mouth, and dizziness [37].

2.2.2 The Clinical Utility of DAT-Scan

The progressive degeneration of nigrostriatal dopaminergic neurons can be assessed by using radioligands in imaging-based approaches. DAT imaging can afford information in patients suspected of having a dopamine deficient degenerative parkinsonian syndrome and discriminate this from alternative diagnoses. It can be useful for assessing whether striatal dopamine deficiency is present in patients with suspected PD who are not responding to therapy as well as it might be hoped. Additionally, it can also potentially be used to detect subclinical striatal dopamine deficiency in subjects at risk for developing PD, even though, in the absence of an effective neuroprotective agent, the value of this remains uncertain [26], [38].

The dimensions of the striatal uptake region, especially the length from the caudate head (most anterior) to the most posterior putamen contours, are key factors in the visual assessment of the ^{123}I-FP-CIT SPECT brain images made by physicians.

For each side of the striatum, the specific binding ratio (SBR) represents the ratio between the counts concentration in the striatum due to the specific binding only and the count concentration in the reference region due to the free and nonspecific binding, and it is given by:

$$SBR = \frac{V_{VX}}{V_s} \times \frac{Ct_{ROI} - R \times V_{ROI}}{R}$$

Where V_{VX} is the volume of a single voxel, V_s is the volume of the striatum, Ct_{ROI} is the total count in the large striatum region of interest (ROI), R is the mean count per voxel within the reference ROI, and V_{ROI} is the volume of the large striatum ROI in numbers of voxels [39], [40].

This medical examination shows whether there is a greater uptake in the putamen (early stages of PD) or in the putamen and caudate (early stages of ET) allowing distinguish PD from ET, for example. Therefore, DAT-Scan provides a potential tool to evaluate patients with unclear PS symptoms, and it also contributes to accurate clinical management of the patient and prevention of unnecessary medications and procedures [25].

2.2.3 The Role of DAT-Scan in the Diagnosis of Parkinson's Disease

As mentioned previously, SPECT imaging using ^{123}I-Ioflupane (^{123}I-FP-CIT SPECT) is commonly used for diagnosis PD, once provides information based on local binding of presynaptic DATs. This binding measure is quantitative and assesses the spatial distribution of DATs. The decrease of ^{123}I-FP-CIT specific uptake in the putamen excludes the diagnosis of other diseases running with no dopaminergic degeneration, such as essential tremor (ET) or drug-induced parkinsonism (DIP) [41]. Consequently, DAT-Scan can differentiate Parkinson's from ET or DIP (movement disorders that do not affect the dopamine cells). When, for example, it's hard to tell whether a person's shaking is from essential tremor or Parkinson's, DAT-Scan may be used to separate the two conditions, which have different treatment options and prognoses [42].

However, any disease that causes loss of presynaptic dopamine neurons will appear as abnormal compared with normal controls. Thus, ^{123}I-FP-CIT SPECT is not able to differentiate among PD, PSP, MSA, CBD and other neurodegenerative disorders that affect the dopamine neurons, which mean DAT-Scan cannot be used on its own to diagnose Parkinson's because conditions other than Parkinson's decrease dopamine activity and cause abnormal images [43], [44].

2.2.4 The Problem of Using DAT-Scan

^{123}I-FP-CIT SPECT is useful for the differentiation of PD from disorders without presynaptic dopaminergic terminal deficiency (e.g. ET or VP) and it is non-invasive. However, it presents some disadvantages.

From a clinical point of view, a factor that weakens the robustness of ^{123}I-FP-CIT SPECT is the fact of its assessment to be made in a subjective visual way. Even though, objectivity may come through a ROI approach or voxel-based techniques that can improve its wide clinical use. In spite of that, it cannot distinguish PD from other disorders associated with SNpc neurodegeneration (e.g. PSP, MSA, CBD or DLB).

From a methodology point of view, there are several methods to quantify ^{123}I-FP-CIT SPECT images that can assist the diagnosis of PSs such as ROIs, one-shape analysis of the uptake, Statistical Parametric Mapping (SPM) analysis based on background ratios, principal component analysis, and machine learning (that can be applied to the SPECT images through computer-aided diagnosis systems).

From a costs point of view, ^{123}I-FP-CIT SPECT is very expensive. But, the cost of SPECT imaging is much less compared to other functional imaging techniques such as Positron Emission Tomography (PET) [34], [45].

2.3 Gait Analysis and Kinematics

Gait analysis studies human locomotion and it is very useful for a better understanding of the mechanisms of movement disorders. It is possible to determine the kinematics and kinetics parameters of human gait through it. It can also estimate physiological gait parameters, i.e., spatiotemporal parameters (cadence, step length, gait asymmetry, etc.), and evaluate quantitatively the musculoskeletal functions [11].

The interest in the analysis of movement and especially in gait analysis began in the ancient times, through observation, by Aristotle, Hippocrates, Galen, Leonardo da Vinci, and Honoré de Balzac to analyse the gait of human beings with [46].

The interest in the analysis of human gait emerged owing to motion analysis, provided information possibly pathological processes that are not directly perceptible except by using deeply invasive procedures [47]. It was only in the second half of the 18th century that were published papers on the biomechanics of human gait [48].

Research on gait analysis has been conducted since the late 19th century, and the general application of gait analysis to humans with pathological conditions such as Parkinson's Disease began in the 1970s, with the technological advances which allowed the production of detailed patient studies [49].

In the last decades, the measuring and recording techniques for capturing gait patterns have improved a lot and gait analysis of human movement. Consequently, gait analysis has its applications presently in almost all significant fields of human locomotion. It has been a fundamental method and assistive tool to characterize human locomotion in the field of biomedical engineering [50], [51].

2.3.1 Gait in Parkinson's Disease

Gait is defined as a pattern of walking. While a "normal gait" is characterized by an upright, by an even stride and by arms swinging at the sides, a "Parkinsonian gait" is defined as having a less steady walk that results from changes in posture, slowness of movement (bradykinesia) and a shortened stride [52].

As discussed previously, the exact diagnosis of PD may be delayed in early stages, as structural neuroimaging methods do not provide characteristic features to allow the diagnosis of PD [53]. In the early stages of PD, many gait alterations become apparent when patients walk or do another task at the same time. These changes are noticeable, for instance, in the gait which is slow, in the step length that shortens, in the reduced arm swing amplitude and the smoothness of movement compared to healthy age-matched people. The symptoms are often unilateral, corresponding to asymmetrical basal ganglia neuropathology. Therefore, gait analysis may help PD diagnosis [54], [56].

Gait analysis can be characterized by biomechanical engineering, which involved the measurement, analysis, and assessment of the biomechanical features that are associated with the walking task [57], and used for two very different purposes: to aid directly in the treatment of individual patients and to improve our understanding of gait through research [50]. It performs an important role in supporting human mobility and it is a relevant tool for obtaining quantitative information on motor deficits in PD, allowing the clinician to assess the degree of abnormality and to reassess the effectiveness of treatment [55], [58]. For this reason, gait analysis needs a biomechanical model that will indicate the positions of the body segments from the areas measured by the markers placed on the skin.

2.3.2 Kinematics and Kinetics

In general, the physical ways to analyse gait are based on kinematics and kinetics. Then, gait analysis is considered an acceptable tool for kinesiology analysis of movement disorders, including for evaluating gait and posture disturbances, once their data are applied to the model for the analysis of gait patterns and behaviour. Kinematics and kinetic data represent fundamentally the locomotion pattern of the human musculoskeletal system in 2D or 3D environment [59], [60].

Kinematics describes the body motion without consideration of the fundamental forces responsible for the movement. It focuses on the study of the relative movement between body segments. Kinematics parameters include measurements of the position and orientation of the body segments, joints angles and the corresponding linear and angular velocities and acceleration [57]. Kinematics data are valuable in the analysis of gait disorders. However, they do not provide information on biomechanical efficiency, ground reaction forces, joint moments, or joint powers. Furthermore, kinematics data can be supplemented with temporal and stride events that include cadence, walking speed, stride time, stride length, step time, step length, period of single limb support, and period of double limb support [48].

A part of kinematic variables control, which is related to planning and decision making, is the *Inverse Kinematics* (IK) problem, which is to calculate the inverse function of the *forward kinematics*. The forward kinematics serves to get coordinate of the end effector from given angles of all joints. Contrary to the forward kinematics problem which is deterministic, the IK problem has no unique solution for a manipulator with several degrees of freedom [61]. Thus, the IK problem will be applied in this study, once it aims at determining the angular kinematic variables in the joint configuration space, based on the Cartesian kinematic variables of the end-effector [62].

On the other hand, kinetics study the motion with consideration of the underlying forces that cause the movement. The kinetics analysis uses reaction forces, joint forces, moments, and powers from the movement and impact of the musculoskeletal system of the

human body. These forces include the external ground reaction forces and the internal joint, muscle, and ligamentous forces [63].

2.3.3 Motion Capture System

Technological advances produced relatively low-cost tools, such as inertial sensors that rapidly replacing complex camera-based motion capture systems, allowing clinicians to quantitatively assess gait. They have been widely applied to the problem of the recognition of the gait where the gait evaluated can be interpreted as a biometric trace [64]–[66].

One of the well-known techniques of gait analysis is the use of motion capture camera. This one can be used to provide comprehensive, objective measurements such as: joint positions, joint motion trajectories, and joint angle variations during walking. However, this equipment is expensive, non-portable, requires a high level of technical expertise and a lengthy calibration process. Usually, the clinicians do not have access to objective biomechanical information for assessing patient performance and as such, the use of these systems is not widespread in clinical practice [57].

A potential solution to this problem is the inertial measurement units (IMUs), which could be used in clinical settings to objectively measure movement patterns during functional activities. These systems are more and more available, from companies such as Xsens Technologies B.V., (Enschede, The Netherlands) and will be used in this study [67],[68].

These IMU are devices constituted by three dimensional (3D) accelerometers and 3D gyroscopes. They are used for the detection of human movements. Accelerometers detect movement, measure the force of acceleration along a given and transforms the mechanical signal into an electric one. They work by two components: Direct current (DC), which senses the gravity effect and uses it to determine the position of the body, and alternating current (AC) that represents the voluntary movement. Gyroscopes are ideal to detect the angular velocity of a rotating body and they are subject to less mechanical noise [69]. When both combined together, turning is better evaluated with less motion dynamic artifact, once accelerometer can be used to compensate the drift of the gyroscope about the axes of the horizontal plane [70]. Therefore, the data from accelerometers and gyroscopes provide the facilities to analyse human locomotion in 3D environment [64].

Compared to motion capture camera the sensors can allow to estimate with great accuracy and reliability the full-body kinematic motion parameters, as well as the position, the speed, and the acceleration produced by the movement. They are small, lightweight, and capable to detect a large range of angular velocity and acceleration, portable and less expensive than traditional camera-based motion-capture systems [70], [72]. However, sometimes it could be difficult to identify the exact length of the segment, rotational axis and different positions of sensor attachments, showing variations in acceleration sensing [64].

The biomechanical models afford a non-invasive means through the IMUs to study human movement and predict the effects of interventions in the gait. These models can deliver different types of relevant information (the 3D body segment kinematics, the spatiotemporal locomotion parameters and the locomotion patterns) in real-time [73]. They can be applied to using some contact points defined through the lowest body models or in the full-body models, for instance.

The lowest body model provides accurate 3D segment orientation estimates for the lowest body based on the inertial motion capture method tracking the 3D kinematics of the pelvis, the upper legs, the lower legs and the feet [74]. The 3D full-body model based on the inertial motion capture method includes 15 segments: head, chest, arms, forearms, hands, pelvis, upper legs, lower legs, and feet [75].

These models allow maintaining a good average 3D kinematics estimation error in the low and the high acceleration locomotion. However, the 3D full-body model can give more information than the lowest limbs model.

3 Methodology

This chapter provides the experimental details for this study. It presents the population dataset, the protocol applied, the DAT-Scan image processing steps, the procedures steps for each data collection and the statistical analysis made. The information about equipment and software are listed in the **Appendix 1** and the **Appendix** , respectively.

3.1 Population Dataset

Twenty-one volunteers participated in the study, being recruited from the Nuclear Medicine Unit in the Champalimaud Clinical Centre (CCC), Lisbon. The general inclusion and the exclusion criteria are listed as follows:

Inclusion Criteria

- Individuals were referred to DAT-Scan for differential diagnosis of parkinsonism;
- ≥18-year-old.

Exclusion Criteria

- Any disorder that could influence walking (e.g. painful arthritis, peripheral neuropathy);
- Any relevant unstable medical condition;
- Use of a walking aid;
- Pregnancy;
- Any contraindication for DAT-Scan (patients referred but found because they have a contraindication like known hypersensitivity either to the active substance, excipients or to iodine).

All participants signed a voluntary consent form. The study was approved by the local ethics committee and by the Code of Ethics of the World Medical Association (Helsinki Declaration).

3.2 Data Collection

3.2.1 Instrumentation

A full body configuration was applied using 15 inertial sensors (MVN BIOMECH Awinda, Xsens Technologies, Enschede, The Netherlands) with dimensions of 47 x 30 x 13 mm, attached with elastic velcro straps positioned throughout the body in order to assess the kinematics. The inertial sensors (MTw Awinda) were placed in a similar way to that illustrated in the **Figure 3.1**. Additionally, a static calibration was performed to align the sensor's orientation to the segment's orientation. This one was done with the participant standing next to the Awinda, with the forearms at a 90º degree angle with the arms and the feet parallel to each other pointing forward. The position, velocity, acceleration data for each segment were then analysed and a set of features of derived were used in the classification system.

Figure 3.1| Example of an individual outfitted with Xsens wearable inertial sensor technology: $(1\times)$ on head, $(1\times)$ on chest, $(2\times)$ on arms, $(2\times)$ on forearms, $(2\times)$ on hands, $(1\times)$ on pelvis, $(2\times)$ on thighs, $(2\times)$ on legs and $(2\times)$ on feet [70].

3.2.2 Feature Extraction

The selection and extraction of appropriate features were important aspects of the research. All the classification results were based on the extracted features. The selected features were independent of the location, the direction and the trajectory of the motion studied. It is reasonable for the gait to deduce that the most important facets to consider would be the legs, the feet and the arms. The features were extracted in a gait cycle for each individual.

The data produced by the MTw Awinda were stored in a rich detail within an MVNX (Moven Open XML format) file which contained the 3D position, the 3D orientation, the 3D acceleration, the 3D velocity, the 3D angular rate and the 3D angular acceleration of each segment.

The extracted features chosen were the subtended angles of the following body elements: head, chest, left and right arm, left and right forearm, left and right hand, pelvis, left and right thigh, left and right ankle and left and right foot. Thirteen features per individual were extracted in the total.

3.2.3 Data Analysis

3.2.3.1 Kinematics

As mentioned in the previous chapter kinematics gait analysis is concerning with the description of gait components. The Link system was used to collect the inertial-based spatiotemporal data, i.e., the distance (spatial) and the time (temporal) parameters. Of the variables that were collected, four of them could be expressed in time (s), four in distance (cm) and the remaining ones in percentage (%).

The time parameters that were collected include the following: the *cycle duration*, which represents the period of time required for an individual to complete a cycle of a lap; the *step duration* that is the period of time required for an individual to take a step; the *cadence* (steps/min) that expresses the number of steps per unit time and the *velocity* (m/s), which characterizes the speed of the path taken by an individual.

Regarding the distance parameters, it was collected the following: the *step length*, which represents the distance between the first point of contact of a limb (feet) with the ground and the first point of contact of the limb on the opposite side; the *step height*; the *step width* that is measure that is perpendicular to each foot midline, between the initial point of contact of one foot and the successive initial point of contact of the opposite foot; and the *arm swing* that is a natural movement where each arm swings with the motion of the opposing leg.

It was also collected from the variables that can be expressed in percentage the following: the *support phase duration*, which refers to reference limb in contact with the floor; the *swing phase duration* that refers to reference limb, not in contact with the floor; the *step duration asymmetry*; *the step length asymmetry* and the *double support phase*, which relate to both feet in contact with the floor.

The three-dimensional acceleration of the inertial sensors was calculated using motion capture data and it was transformed into the sensor coordinate system. Then these data were time-matched to within 0.01 s of the corresponding raw sensors accelerometers data. It was used a custom semi-automatic correlation method which used the cross-correlation to provide an initial guess and then manual adjustment to find the final synchronization point.

It was applied the inverse kinematics (IK) instead of forward kinematics because this one permits to calculate the correct angles for a desirable position and orientation. Therefore, the IK allows to reconstruct the 3D biomechanical model.

3.2.3.2 DAT-Scan

Firstly, the images were registered in ITK-SNAP library. Next, four regions of interest (ROIs) were defined: a large ROI over the whole nonspecific brain region that was used as the reference region, and three ROIs on each hemisphere of the brain: one over the putamen ,another one over the caudate and one large ROI containing the entire striatum and surrounding area, as shown in the **Figures 3.2** and **3.3.**

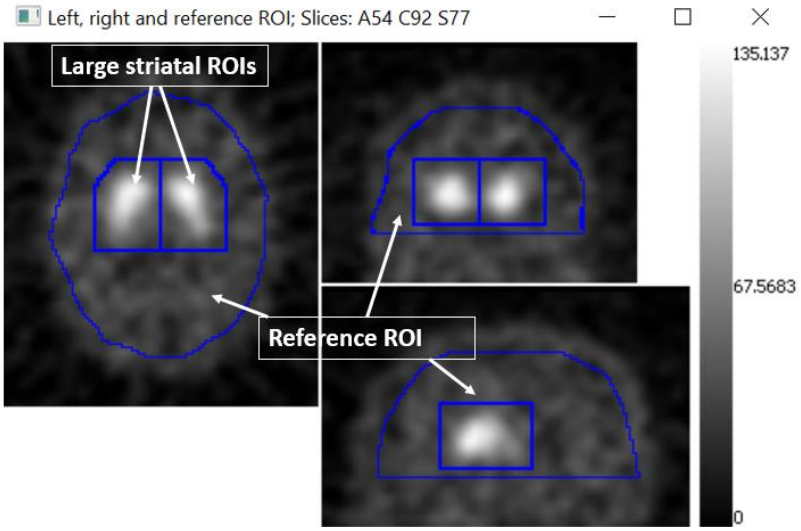

Figure 3.2| Example of striatal large ROI and reference ROI visualization: on the left, an axial plane; **middle top**, a coronal plane; **middle bottom**, a sagittal plane, and **on the right**, the scale represents the number of counts per voxel.

The shape of these ROIs and their inferior-superior position in the brain were established based on the SPECT template.

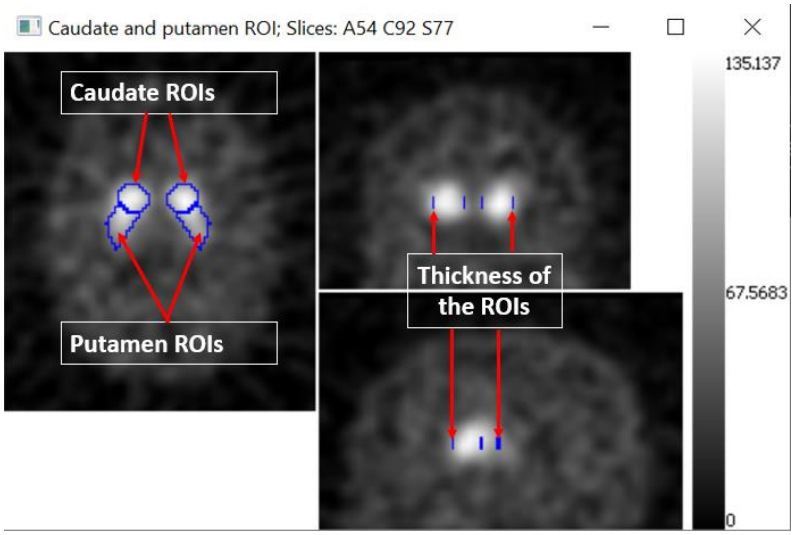

Figure 3.3 | Example of caudate and putamen 3D ROIs visualization: on the left, an axial plane; **middle top**, a coronal plane; **middle bottom**, a sagittal plane, and **on the right,** the scale represents the number of counts per voxel.

The computation of the striatal uptake ratios was calculated as well. Then it was built the voxel-wise binding potential image and it was done the assessment of the dimensions of the striatal uptake region. Finally, the feature vectors were assembled to be used in the classification.

In the end, if there was a normal uptake, this classification would detect a normal pattern similar to a healthy control, or if uptake was abnormal, the classification would detect an abnormal pattern based on the standardized patterns of PD.

The results of the DAT-Scan were defined qualitatively and quantitatively. They were classified qualitatively by the responsible physician for the nuclear medicine unit from the CCC, and quantitatively by the classification referred above that confirms the diagnoses made qualitatively. In this way it was possible to create two different labels: individual without denervation and individual with denervation, respectively.

The features from the striatum used to help determining, whether there was dopamine uptake or not , were the following ones: Uptake ratio-based features (specific binding ratio (SBR), caudate binding potential (CBP), putamen binding potential (PBP), striatum binding potential (SBP) and putamen-to-caudate ratio (PCR)) along with dimensional features related to the volume, width, length, and thickness. The automated computation of the uptake ratios was based on the counts inside the volumetric ROIs placed

over the registered image under study. The BP_{ND} referred to the ratio at equilibrium of specifically bound radioligands to the non-displaceable ones in tissue, and it encompassed three regions: the CBP, the PBP and the SBP.

BP_{ND} was given by $BP_{ND} = (V_T - V_{ND}) / V_{ND}$, where V_T was the radioligands volume of distribution of the target region and V_{ND} was the sum of the volume of distribution of the free and non-specifically bound ligand. Since V_T and V_{ND} were directly proportional to the counts per voxel of the target and reference regions, respectively, then CBP = (C - R) / R, PBP = (P - R) / R, and SBP = (S - R) / R, where C was the mean count per voxel in the caudate ROI, R was the mean count per voxel within the reference region, P was the mean count per voxel in the putamen ROI and S was the mean count per voxel in the striatum (caudate and putamen ROIs). The PCR was also computed and it was given by PCR = PBP/CBP.

The literature suggested the binding potential could be defined at the voxel level as $BP_{ND} = [I(x,y,z) – R] / R$, where I (x,y,z) was the count associated to the voxel with coordinates (x,y,z), and R was the mean count per voxel within the reference ROI [40]. The **Figure 3.4** shows an example of a BP_{ND} image built.

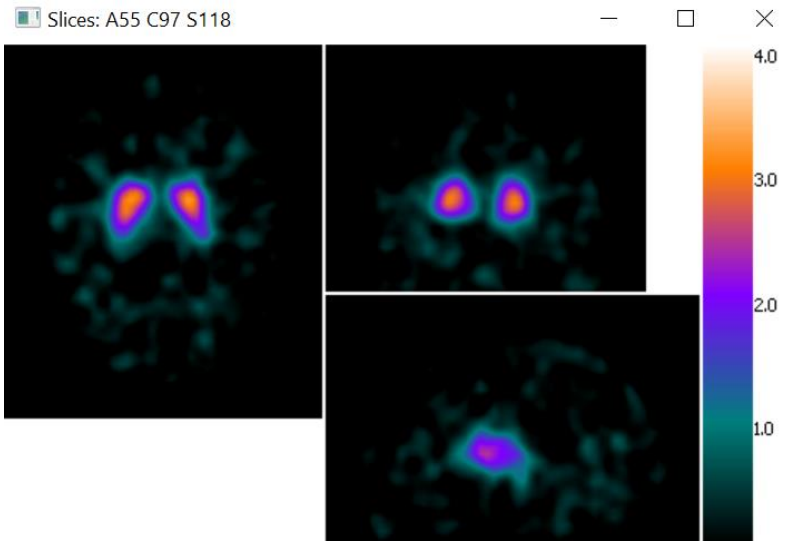

Figure 3.4 | Example of a BP_{ND} image built from a subject without denervation: On the left, an axial slice is visible; **middle top**, a coronal slice; **middle bottom**, a sagittal slice; and **on the right**, the dimensionless BP_{ND} colour scale used (only voxels with a positive BP_{ND} are shown).

The extraction of the region with uptake was performed on the BP_{ND} image, and it was based on a cut-off level, which means that only voxels with a BP_{ND} higher than the cut-off level defined were included in the segmented region. After the initial cut-off, the binary image obtained was cleaned of scattered voxels by selecting only the larger group of connected voxels in each hemisphere. The total volume of the two sides of the segmented striatal region and the corresponding lengths were automatically calculated from the segmented image based on the orientation established for the template image as illustrated in the

Figure 3.5. When there were no voxels with BP_{ND} greater than the cut-off level defined, the dimensional features were set to zero.

The optimal cut-off level was chosen based on the classification accuracy, i.e. the cut-off value that originated the best discrimination between without denervation and with denervation patients using the volume and length dimensional measures was chosen.

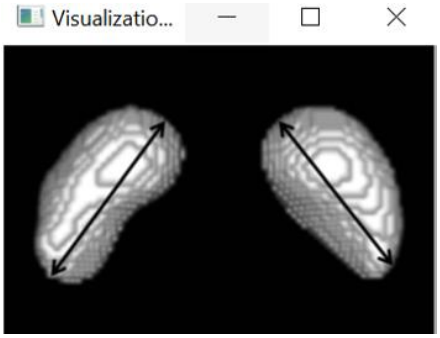

Figure 3.5| Example of the segmented region with normal uptake obtained from a subject without denervation. The arrows indicate the directions defined for measuring the length.

3.3 Procedures

The procedures included:

i. Assembling the equipment for data collection;
ii. The Injection: all participants were first injected with ^{123}Ioflupane. After that, the participants were approached and it was explained what our study consisted of. Then they were invited to participate;
iii. The individuals, who accepted to participate, signed the consent form at the nuclear medicine unit at the same place where they had been injected (CCC), being then headed for a corridor that was used for the assessment (with two red marks on the floor indicating the start and the end of the meters that the participants had to walk);
iv. MDS-UPRDS-III scale evaluation;
v. Equipping the participants with the inertial sensors (with dimensions of 47x30x13mm and a sampling rate of 1000Hz);
vi. The sensors were synchronized (time-synchronization ≤10 μs), and calibrated before starting collecting;
vii. The next step was to instruct the participants to stay still in orthostatic position, first with the feet as close together as possible and then with both feet shoulder-width apart, for postural control acquisition. The arms persisted motionless along the body and eyes fixed at a point ahead. The participants were instructed to

keep their posture for one acquisition of 30s each with eyes open. The participants performed three walking trials for kinematics gait acquisition, in a straight line along a 15m x2 long walkway without any assistance;

viii. Unequipping the participants and taking them back to nuclear medicine unit;

ix. ^{123}I-FP-CIT SPECT (DATScan^{TM}): Dopamine Transporter (DAT) imaging was assessed through DATScan performed at the Nuclear Medicine Unit in CCC. SPECT scans lasted from 30 to 45 min and they started post-injection of activity between 110 and 185 MBq.

x. Disassembling the equipment for data collection.

3.4 Statistical Analysis

The Statistical analysis was performed using IBM Statistical Package for the Social Sciences (SPSS Statistics) Version 22.0. The data analysis presented was carried out in demographic data that were assumed as independent observations and they were tested with the t-test because they were continuous variables.

Secondly, it was compared the means of the lowest specific binding ratio (SBR) of denervated individuals with the highest SBR of non-denervated individuals because an individual with denervation is not equal in the both sides, thus avoiding having inflated values. There is one side that is worse than the other one. However, a person can have a good side, i.e., a normal one. It was also compared the best brain sides, as well as the asymmetries indexes of the DAT-Scan variables, through the independent t-tests to determine whether there was a statistically significant difference between the means in the two groups (the patients with and without denervation). The same procedure was applied to the kinematics data. It was established a significance level of 0.05.

It was also made a Pearson correlation to determine associations just for the group of individuals with denervation between the ^{123}I-FP-CIT SPECT (DAT-Scan) and the kinematic variables, and between the MDS-UPDRS III and the kinematic variables. The reliability of the joint angles was determined based on the correlation coefficient (r), including the 95% confidence interval. The correlations were classified as very strong (0.9-1.0), strong (0.7-0.9), moderate (0.5-0.69), weak (0.3-0.49) and negligible (<0.30) based on [76].

4 Results

The aim of this work is to discover if kinematics can give the same information as the DAT-Scan. It will be made a description of the main outcomes from clinical and demographic data to the associations between DAT-Scan, kinematics and MDS-UPDRS III (motor symptoms), throughout this chapter.

4.1 MDS-UPDRS III subscores

Twenty-one patients participated in this study, being recruited from the Nuclear Medicine Unit in the Champalimaud Clinical Centre (CCC), Lisbon. Within these 21 patients, 10 of them had denervation (mean age, 68.4 ± 7.8 years) and the remaining 11 (mean age, 66.6 ± 7.4 years) did not present denervation.

According to what was described in section 2.1.3, the Movement Disorder Society-Unified Parkinson Disease Rating Scale (MDS-UPDRS III) was subdivided into 4 subscores: tremor, rigidity, bradykinesia and axial. The demographic and clinical characteristics of all study participants are displayed in the **Table 4.1**.

Table 4.1: Demographic and clinical characteristics of all participants.

	Individuals with denervation (n = 10)	**Individuals without denervation (n = 11)**	***p -value***
Male	3	4	
Female	7	7	
	Mean ± Std	**Mean ± Std**	
Age (years)	68.4 ± 7.8	66.6 ± 7.4	0.809[a]
LED (mg)	273.0 ± 313.0	139.5 ± 214.9	0.057[a]
Total MDS-UPDRS III score	29.0 ± 16.2	15.3 ± 10.3	0.072[a]
Sum of axial subscore	7.6 ± 3.7	4.0 ± 3.6	0.045*[a]

Sum of bradykinesia subscore	4.4 ± 4.4	2.1 ± 1.9	0.052[a]
Sum of rigidity subscore	13.2 ± 4.1	6.8 ± 3.4	0.034*[a]
Sum of tremor subscore	5.0 ± 1.4	3.1 ± 1.9	0.047*[a]
Duration of Motor Symptoms (months)	85.8 ± 80.9	29.2 ± 11.7	0.017*[a]

Abbreviations:

Clinical features: LED Levodopa Equivalent Dose, MDS UPDRS Movement Disorder Society Unified Parkinson's Disease Rating Scale.

Others: Std Standard Deviation, n sample size.

Data are expressed as mean ± standard deviation.

[a=] t test (p <0.05 - *Statistically significant difference).

4.2 Distinction between normal and abnormal from DAT-Scan

As it was explained in chapter 2, it was given a normal interpretation regarding to DAT-Scan if there was a homogeneous symmetrical comma type pattern in the striatum (normal DAT-Scan – individual without denervation). Another pattern was interpreted as abnormal, indicating a PS (abnormal DAT-Scan – individual with denervation). An illustrative DAT-Scan is shown in **Figure 4.1:** normal **(A)** and abnormal **(B)**.

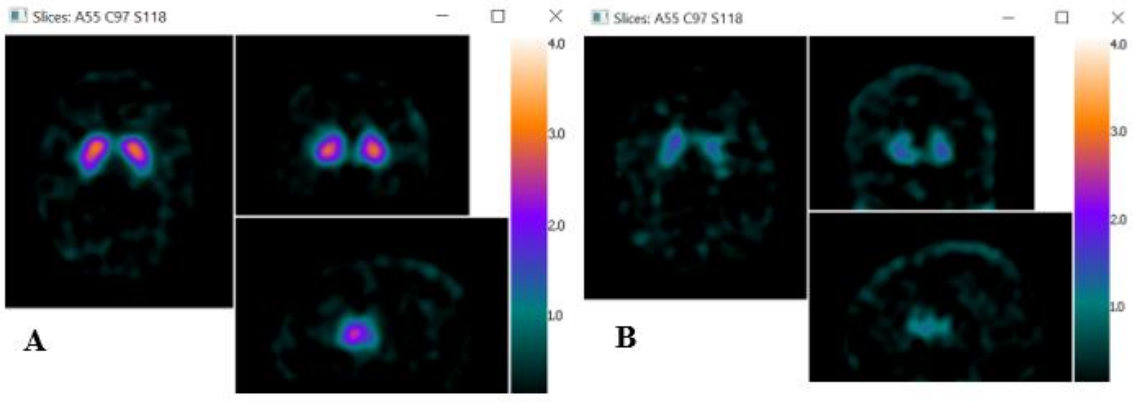

Figure 4.1| Representative DAT-Scan: **(A)** normal - the striatum has a comma shape; **(B)** abnormal – the striatum has not a comma pattern.

For each patient the specific binding ratio (SBR) was compared and sides were grouped based on lower SBR (more denervation) of high SBR (less denervation). It was also compared the asymmetries indexes in order to observe differences between a normal DAT-Scan (individuals without denervation) comparatively to abnormal DAT-Scan (individuals with denervation).

The comparative analysis between the lower SBR sides of abnormal and normal ^{123}I-FP-CIT SPECT (DAT-Scan) are presented in **Table 4.2**. The values statistically significant are in bolt. The results showed that the lower SBR side values of uptake ratio-based features and dimensional features related to the volume, width, length, and thickness in individuals with dopamine depletion in the striatum (abnormal DAT-Scan) are inferior regarding to the lower SBR side in individuals without dopamine depletion.

Table 4.2: Clinical data of the lower SBR sides of an abnormal and a normal DAT-Scan.

	Abnormal DAT-Scan / Individual with denervation (n = 10)	**Normal DAT-Scan / Individual without denervation (n = 11)**	***p-value***
	(Mean ± Std)	(Mean ± Std)	
SBR (a.u.)	2.99 ± 0.07	4.58 ± 1.13	**0.004*[a]**
CBP (a.u.)	1.39 ± 0.03	1.99 ± 0.32	**<0.001[a]**
PBP (a.u.)	0.68 ± 0.04	1.46 ± 0.29	**<0.001[a]**
SBP (a.u.)	1.02 ± 0.05	1.72 ± 0.29	**<0.001[a]**
PCR (a.u.)	0.49 ± 0.08	1.71 ± 0.09	**0.003*[a]**
Volume (mm^3)	1763.75 ± 780.18	6892.72 ± 3074.97	**0.001*[a]**
Width (mm)	11.33 ± 0.52	19.15 ± 2.92	**0.001*[a]**
Length (mm)	11.80 ± 0.36	32.17 ± 4.63	**0.001*[a]**
Thickness (mm)	13.52 ± 0.04	22.81 ± 3.16	**0.009*[a]**

Abbreviations:
Uptake ratio features: SBR Specific Binding Ratio, CBP Caudate Binding Potential, PBP Putamen Binding Potential, SBP Striatum Binding Potential, PCR Putamen to Caudate Ratio.
Others: a.u. arbitrary units, n sample size.
Data are expressed as mean ± standard deviation.

[a]=t test: *lower SBR sides* of abnormal vs. normal DAT-Scan (p <0.05 - *Statistically significant difference).

The means and respective standard deviations of each side of the brain, as well as the comparative analysis between the high SBR sides of these two groups can be seen in **Appendix 3 (Table 8.3 and Table 8.4)**, respectively.

The comparative analysis between the asymmetry indexes of the abnormal and the normal DAT-Scan are presented in **Table 4.3**. The values statistically significant are in bold. The results showed that the asymmetry indexes in the abnormal DAT-Scan are higher than in the normal DAT-Scan. Significant differences are also identified between the groups in all features.

Table 4.3: Clinical data of asymmetry indexes between normal and abnormal DAT-Scan.

	Abnormal/With denervation (n = 10)	**Normal/Without denervation (n = 11)**	
	Asymmetry index (Mean ± Std)	Asymmetry index (Mean ± Std)	*p-value*
SBR (a.u.)	0.35 ± 0.10	0.01 ± 0.03	**0.002*[a]**
CBP (a.u.)	0.18 ± 0.69	0.03 ± 0.04	**<0.001[a]**
PBP (a.u.)	0.33 ± 0.19	0.28 ± 0.09	**<0.001[a]**
SBP (a.u.)	0.17 ± 0.40	0.04 ± 0.66	**<0.001[a]**
PCR (a.u.)	2.23 ± 1.11	2.25 ± 1.30	**<0.001[a]**
Volume (mm^3)	0.57 ± 0.23	0.06 ± 0.02	**0.001*[a]**
Width (mm)	2.15 ± 1.23	0.10 ± 0.06	**0.001*[a]**
Length (mm)	2.23 ± 1.54	2.08 ± 0.45	**<0.001[a]**
Thickness (mm)	1.92 ± 0.21	0.27 ± 0.66	**0.008*[a]**

Abbreviations:
Uptake ratio features: SBR Specific Binding Ratio, CBP Caudate Binding Potential, PBP Putamen Binding Potential, SBP Striatum Binding Potential, PCR Putamen to Caudate Ratio.
Others: a.u. arbitrary units, n sample size.
Data are expressed as mean ± standard deviation.

[a]=t test: asymmetry indexes of abnormal vs. normal DAT-Scan (p <0.05 - *Statistically significant difference).

4.3 Distinction between normal and abnormal from Kinematics

As referred in section 3.2 the kinematics results were based on the extracted spatiotemporal features. The following table (**Table 4.4**) presented display the mean values of the kinematics data collected statistically, based on denervated and non-denervated individuals.

Table 4.4: Statically summary of the gait spatiotemporal parameters.

	Individual with denervation (n = 10)	**Individual without denervation (n = 11)**
	(Mean ± Std)	**(Mean ± Std)**
Cycle duration (s)	1.14 ± 0.15	1.14 ± 0.16
Support phase dur (%)	68.35 ± 12.93	67.31 ± 12.27
Swing phase dur (%)	31.65 ± 2.93	32.69 ± 2.27
Cadence (steps/min)	108.2 ± 12.78	106.7 ± 16.00
Step duration (s)	0.57 ± 0.07	0.56 ± 0.05
Step duration as (%)	1.63 ± 1.53	1.68 ± 1.46
Step length (cm)	45.32 ± 11.72	48.60 ± 9.33
Step length as (cm)	3.74 ± 3.43	3.66 ± 2.54
Step height (cm)	3.97 ± 2.59	5.10 ± 2.09
Step width (cm)	14.79 ± 5.21	11.18 ± 6.41
Gait speed (m/s)	0.84 ± 0.30	0.88 ± 0.12
Double support ph (%)	18.35 ± 3.21	16.33 ± 2.60
Arm swing (cm)	39.79 ± 20.42	43.83 ± 18.20

Abbreviations:

Kinematics variables: Support phase dur Support phase duration, Swing phase dur Swing phase duration, Step duration as Step duration asymmetry, Step length as Step length asymmetry, Double support ph Double support phase.

Others: n sample size.
Data are expressed as mean ± standard deviation.

In agreement with the worst side of DAT-Scan (lower SBR in the striatum), there is also the worst side of the body. This association manifests on opposite sides, i.e., if the affected side of the brain is the right side, then these changes will be visible on the left side of the body and vice versa. Here the worst side is defined by a decrease in the support and the swing phase duration. It is also set by a step duration, length, and height, as well as an arm swing reduced.

The **Table 4.5** presents a comparative analysis between the worst sides of the bilateral variables of the denervated and non-denervated individuals. It shows that the worst side of the denervated individuals is not different from the worst side of the non-denervated individuals, once no significant differences were found in none of the parameters observed.

***Table 4.5**:* Kinematics data of the Worst side of the body in individuals with and without denervation.

	Individual with denervation (n = 10)	**Individual without denervation (n = 11)**	***p-value***
	(Mean ± Std)	(Mean ± Std)	
Support phase dur (%)	68.39 ± 2.80	68.20 ± 1.67	0.591[a]
Swing phase dur (%)	31.61 ± 2.80	31.80 ± 2.65	0.591[a]
Step duration (s)	0.57 ± 0.07	0.58 ± 0.05	0.694[a]
Step length (cm)	42.78 ± 12.09	46.46 ± 4.92	0.616[a]
Step height (cm)	3.36 ± 2.81	4.57 ± 2.09	0.363[a]
Arm swing (cm)	36.00 ± 16.83	43.32 ± 12.29	0.539[a]

Abbreviations:

Kinematics variables: Support phase dur Support phase duration, Swing phase dur Swing phase duration.

Others: n sample size.
Data are expressed as mean ± standard deviation.

[a=]t test: worst side of individuals with denervation vs. individuals without denervation, (p <0.05 - *Statistically significant difference).

The means and respective standard deviations on either body's side (left and right) of the collected biomechanical parameters, as well as the comparative analysis between the best sides of the body between these two groups can be seen in **Appendix 4 (Table 8.5 and Table 8.6)**, respectively.

The following table (**Table 4.6**) shows that regarding to the asymmetry indexes no significant differences were found between the individuals with denervation and the individuals without denervation.

Table 4.6: kinematics comparison of asymmetry indexes between individuals with and without denervation.

	Individuals with denervation (n = 10)	**Individuals without denervation (n = 11)**	
	Asymmetry index (Mean ± Std)	Asymmetry index (Mean ± Std)	*p-value*
Support phase dur (%)	0.57 ± 0.39	1.01 ± 0.66	0.064[a]
Swing phase dur (%)	0.88 ± 0.69	0.71 ± 0.57	0.698[a]
Step duration (s)	1.55 ± 0.07	0.16 ± 0.05	0.041*[a]
Step length (cm)	0.51 ± 0.27	0.10 ± 0.33	0.888[a]
Step height (cm)	0.74 ± 0.59	0.90 ± 0.66	0.397[a]
Arm swing (cm)	0.69 ± 0.25	0.50 ± 0.26	0.647[a]

Abbreviations:
Kinematics variables: Support phase dur Support phase duration, Swing phase dur Swing phase duration.
Others: n sample size.
Data are expressed as mean ± standard deviation.

[a] = t test: Asymmetry indexes between individuals with and without denervation, ($p < 0.05$ - *Statistically significant difference).

4.4 Patients with Denervation

As it was observed, in kinematics there are no significant differences between the worst and best sides, as well as in the asymmetries between the individuals with and without dopaminergic depletion. So, it was performed an exploratory analysis in the individuals who presented denervation.

4.4.1 Correlation between DAT-Scan and Kinematics

To determine the intensity of the relationship between the DAT-Scan and the kinematics, it was made a Pearson correlation between these two groups. This correlation analysis was performed in the two hemispheres of the brain with the two sides of the body, i.e., the right hemisphere (DAT-Scan R) with the left part of the body (Kinematics L) vs. the left hemisphere (DAT-Scan L) with the right part of the body (Kinematics R). The **Table 4.7** shows the strength of the relationship between the DAT-Scan and the kinematics, which is indicated by the correlation coefficient (r), and it also shows the significance of this relationship that is expressed in probability levels, through the *p*-value (*p*). The significance in a correlation is greater the larger the difference between the sample, that is, the more the sample statistic deviates from the population parameter.

Overall, the results demonstrated that the variables have negligible statistically significant differences. The scatterplots of these correlations are presented in **Appendix 5** (**Figures8(A)-(I)**).

Table 4.7: Correlation matrix of DAT-Scan (R) + kinematic (L) and DAT-Scan (L) + kinematic (R). 1st row/column: SBR (a.u) vs Support phase duration (%); 2nd row/column: CBP (a.u) vs Swing phase duration (%); 3rd row/column: PBP (a.u.) vs Step duration (s) and so on.

		SBR (a.u.)	CBP (a.u.)	PBP (a.u.)	SBP (a.u.)	PCR (a.u.)	Volume (mm^3)	Width (mm)	Length (mm)	Thickness (mm)
Support phase duration (%)	r	0.042	0.163	-0.113	0.135	-0.161	0.104	0.051	0.049	0.090
	p	0.804	0.990	0.385	0.727	0.230	0.775	0.848	0.955	0.938
Swing phase duration (%)	r	-0.135	-0.163	0.113	-0.127	0.161	-0.088	-0.051	-0.049	-0.028
	p	0.804	0.990	0.385	0.727	0.230	0.775	0.848	0.955	0.938
Step duration (s)	r	0.000	0.044	-0.218	0.171	-0.236	0.072	0.085	0.052	0.192
	p	1.000	0.903	0.545	0.742	0.512	0.555	0.793	0.886	0.970
Step length (cm)	r	0.063	0.092	0.243	0.160	0.181	0.209	0.146	0.118	0.066
	p	0.863	0.801	0.499	0.658	0.618	0.562	0.686	0.745	0.856
Step height (cm)	r	-0.375	-0.182	0.259	-0.006	0.566	-0.117	-0.029	-0.056	-0.097
	p	0.461	0.614	0.469	0.986	0.088	0.748	0.937	0.878	0.790
Arm swing (cm)	r	-0.455	-0.368	-0.087	-0.272	0.276	-0.104	-0.339	-0.259	-0.318
	p	0.223	0.296	0.811	0.446	0.440	0.775	0.461	0.470	0.370

Abbreviations:

Uptake ratio features: SBR Specific Binding Ratio, CBP Caudate Binding Potential, PBP Putamen Binding Potential, SBP Striatum Binding Potential, PCR Putamen to Caudate Ratio. Others: r Pearson Correlation, *p* *p*-value, a.u. arbitrary units. * Statistically significant difference

4.4.2 Correlation between Kinematics and MDS-UPDRS III

The correlation analysis shown in **Table 4.8** was performed in the kinematics and MDS-UPDRS III. According to this analysis, UPDRS motor scores revealed a significant negative correlation with (**A**) swing phase duration ($r = -0.781$, $p = 0.041$), (**B**) step length ($r = -0.832$, $p = 0.003$) and (**C**) gait speed ($r = -0.849$, $p = 0.002$, **Figure 4.2**). This means that the higher motor symptoms are, the more time is the swing phase duration and the step length, and the worse is the gait speed.

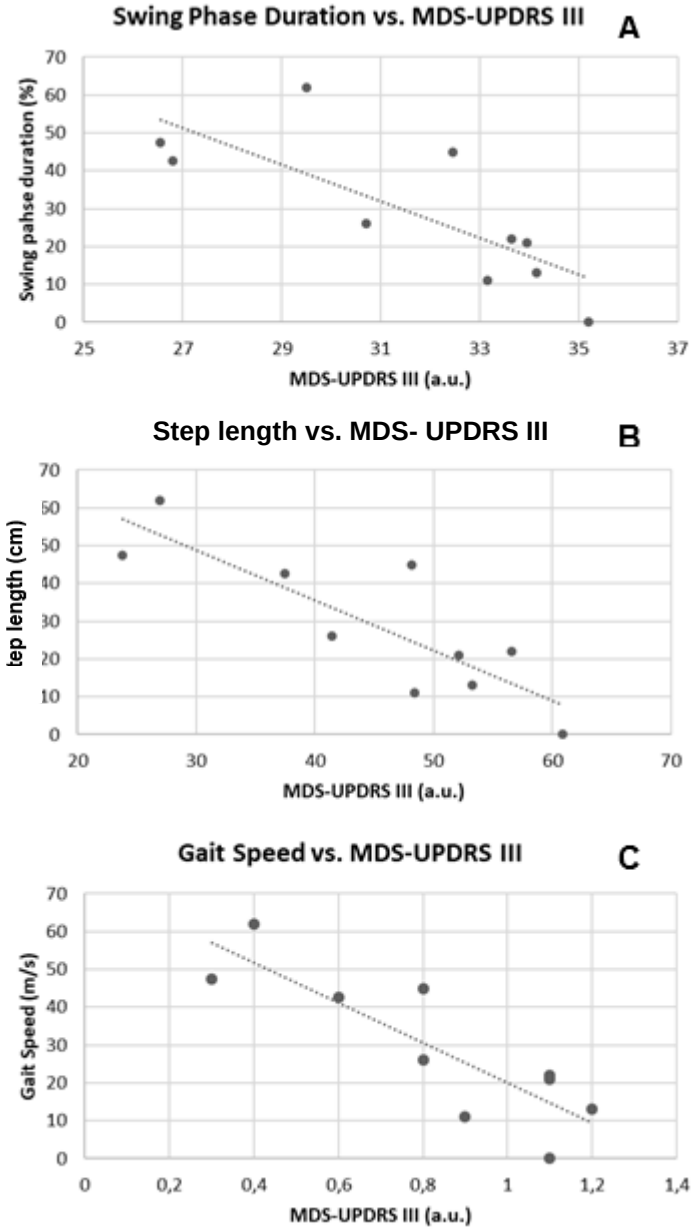

Figure 4.2| Scatterplot of kinematic variables with a significant negative correlation for individuals with denervation: (A) Swing phase duration (%) vs MDS-UPDRS III; **(B)** Step length (cm) vs MDS-UPDRS III; **(C)** Gait speed (m/s) vs MDS-UPDRS III.

The results also showed that cadence has a negative moderate correlation with UPDRS motor scores (r = -0.651, $p = 0.014$), and cycle duration (r = 0.638, $p = 0.047$), support phase duration (r = 0.714, $p = 0.014$), double support phase (r = 0.734, $p = 0.016$) and double support phase.1 (r = 0.645, $p = 0.044$) showed a positive moderate correlation with UPDRS motor scores. That means that the more severe are the motor symptoms, the higher is the support phase duration, the more is the double support phase and the double support phase.1.

Table 4.8: Correlation matrix of MDS-UPDRS III and biomechanical parameters. 1st row/column: cycle duration vs MDS-UPDRS III; 2nd row/column: Support phase duration vs MDS-UPDRS III; 3rd row/column: swing phase duration vs MDS-UPDRS III; (…) 14th row/column: Arm swing vs MDS-UPDRS III.

Individuals with denervation (n=10)

Correlation coefficient		Cycle duration (s)	Support pha dur (%)	Swing pha dur (%)	Cadence (steps/min)	Step duration (s)	Step DAs (%)	Step Length (cm)	Step LAs (%)	Step height (cm)	Step width (cm)	Gait speed (m/s)	Double support ph (%)	Double supp ph1(%)	Arm swing (cm)
MDS-UPDRS III	r	**0.638***	**0.714***	**-0.781****	**-0.651***	0.534	-0.101	**-0.832****	0.590	-0.374	0.356	**-0.849****	**0.734***	**0.645***	-0.509
	p	**0.047***	**0.014***	**0.008***	**0.041***	0.112	0.781	**0.003***	0.072	0.287	0.312	**0.002***	**0.016***	**0.044***	**0.133***

Abbreviations:

Kinematics variables: Support pha dur Support phase duration, Swing pha dur Swing phase duration, Step DAs Step duration asymmetry, Step LAs Step length asymmetry, Double support ph Double support phase, Double supp ph1 Double support phase 1.

Others: n sample size.
r Pearson Correlation, *p* *p*-value.

*Statistically significant difference (p <0.05).
* Correlation is significant at level 0.05
** Correlation is significant at level 0.01

5 Discussion

It was investigated, in this study, the role of the inertial sensors in distinguishing between the denervated and the non-denervated individuals. When we defined "clinically" denervation, quantitatively we had results in line with this. The results presented in the section 4.1 confirmed that the DAT-Scan could distinguish these two groups because significant differences were found between the lowest specific binding ratio (SBR) and the highest SBR (appendix 3) sides of the striatum in both the denervated and the non-denervated individuals. Significant differences were also found in the asymmetry indexes, of the striatum, between these two groups. However, according to the results presented in the section 4.2, the classic spatiotemporal kinematics measures could not distinguish between the denervated and the non-denervated individuals.

Interestingly, we found that kinematics was highly correlated with the classic clinical motor assessment (MDS-UPDRS III) in the patients presenting dopaminergic denervation (independently of the diagnosis) we've found that kinematics was highly correlated with the classic clinical motor assessment (MDS-UPDRS III). This means that, in non-healthy individuals, the full body kinematics (FBK) metrics capture dimension that have been defined by the neurological community as relevant in the assessment of Parkinsonian conditions. Therefore, FBK can have a role in human movement assessment.

It wasn´t found any correlation by the comparison between kinematics metrics and the DAT-Scan quantitative results. This may lead to the hypothesis that a non-linear relationship between motor impairment and dopaminergic denervation exist across Parkinsonian disorders.

The fact that these results are not showing this relationship can have several explanations: the DAT-Scan is very noisy and it does not measure the dopamine (DA), instead of that it measures the availability of the presynaptic dopamine transporters (DATs). This can be overcome by the fluorodopa - F-DOPA, a fluorinated form of levodopa -L-DOPA for use as a radiotracer. In fact, it is known that the motor symptoms in the PD only start after the striatal denervation reaches 70%. Besides this, there are compensation systems in the brain whereby the progression can be nonlinear. At the same time, patients are having symptomatic drugs. These are some of the factors that may have influenced our results.

The results also showed that there was a considerable asymmetry on the upper limbs in both denervated and non-denervated individuals. What make us think that these kinematic variables should be better explored.

Our study has some limitations that must be considered, such as the small sample size. There are also many variables. However, we included individuals whose diagnosis is unknown.

6 Conclusions and Future Perspectives

Walking is fundamental to everyday functioning and independence, and the Parkinson's disease (PD) affects particularly this ability. A better understanding of the reasons and ways can provide information that may be helpful for future research on the motor (MS) and non-motor (NMS) symptoms of the PD that can cause impact in the gait. Moreover, the quantitative measurements of the gait parameters have become available in the clinic, thanks to the reduced size and the low-cost technologies (e.g. inertial sensors).

As main topic, the role of inertial sensors in distinguishing between the denervated and the non-denervated individuals, has been investigated in this dissertation. The main finding is that no differences were found in the classic kinematics metrics between the two groups (the denervated and the non-denervated individuals). However, the kinematics correlated with what the clinician saw in the patients, but it did not correlate strongly with the DAT-Scan. The kinematics took the metrics form the movement, which were considered relevant by the clinicians, but it did not relate linearly to the DAT-Scan results.

These results made us think that it may exist other extractable variables that allow us to distinguish between these two groups, such as the olfactory system variable. Thus, future research should focus on nonlinear metrics to detect denervation in the early stages of Parkinson's disease.

7 References

[1] J. A. Opara, A. Malecki, E. Malecka, and T. Socha, "Motor assessment in Parkinson`s disease," *Ann. Agric. Enviromental Med.*, vol. 24, no. 3, pp. 411–415, 2017.

[2] "Parkinson's Disease vs. Parkinsonmis," *Parkinson's Foundation*, 2018. [Online]. Available: www.parkinson.org. [Accessed: 12-Aug-2019].

[3] D.Verbaan, et al., "Patient-reported autonomic symptoms in Parkinson disease," *Neurology*, vol. 69, no. 4, pp. 333–341, 2007.

[4] J. J. Ferreira, N. Gonçalves, A. Valadas, C. Januário, M. R. Silva, L. Nogueira, "Prevalence of Parkinson's disease : a population-based study in Portugal," *Eur. J. Neurol.*, vol. 0, pp. 1–3, 2017.

[5] C. M. Lill, "Genetics of Parkinson's disease," *Mol. Cell. Probes*, vol. 147, pp. 211–227, 2016.

[6] K. Wirdefeldt, H. O. Adami, P. Cole, D. Trichopoulos, and J. Mandel, "Epidemiology and etiology of Parkinson's disease: a review of the evidence," *Eur J Epidemiol*, vol. 26, 2011.

[7] M. Rodr, R. Zerón-Martínez, A. Cervantes-Arriaga, and T. Corona, "Who Can Diagnose Parkinson's Disease First ? Role of Pre-motor Symptoms," *Elsevier,* vol. 48, pp. 221–227, 2017.

[8] S. R. Suwijn, C. J. M. Van Boheemen, R. J. De Haan, G. Tissingh, J. Booij, and R. M. A. De Bie, "The diagnostic accuracy of dopamine transporter SPECT imaging to detect nigrostriatal cell loss in patients with Parkinson's disease or clinically uncertain parkinsonism : a systematic review," *SpringerOpen J.*, vol. 5, pp. 1–8, 2015.

[9] K. Bötzel, A. Olivares, J. P. Cunha, J. M. Górriz Sáez, R. Weiss, and A. Plate, "Quantification of gait parameters with inertial sensors and inverse kinematics," *J. Biomech.*, vol. 72, pp. 207–214, 2018.

[10] N. Chastan and L. M. Decker, "Posturo-locomotor markers of preclinical Parkinson's disease," *Neurophysiol. Clin.*, vol. 49, no. 2, pp. 173–180, 2019.

[11] W. Tao, T. Liu, R. Zheng, and H. Feng, "Gait Analysis Using Wearable," *Sensors*, vol. 12, no. 2, pp. 2255–2283, 2012.

[12] M. Sancandi, E. V. Schul, G. Economides, A. Constanti, and A. Mercer, "Structural changes observed in the piriform cortex in a rat model of pre-motor Parkinson's disease.," *Front. Cell. Neurosci.*, vol. 12, no. December, p. 479, 2018.

[13] D. N. Hauser and T. G. Hastings, "Mitochondrial dysfunction and oxidative stress in Parkinson's disease and monogenic parkinsonism," *Neurobiol Dis*, vol. 51, pp. 35–42, 2014.

[14] D. S. W. Djang *et al.*, "SNM Practice Guideline for Dopamine Transporter Imaging with 123I-Ioflupane SPECT 1.0," *J. Nucl. Med.*, vol. 53, no. 1, pp. 154–163, 2012.

[15] G. W. Ross *et al.*, "Parkinsonian signs and substantia nigra neuron density in decendents elders without PD," *Ann. Neurol.*, vol. 56, no. 4, pp. 532–539, 2004.

[16] C. A. Davie, "A review of Parkinson's disease," *Br. Med. Bull.*, vol. 86, no. 1, pp. 109–127, 2008.

[17] D. Scherman, C. Desnos, F. Darchen, P. Pollak, F. Javoy-Agid, and Y. Agid, "Striatal dopamine deficiency in parkinson's disease: Role of aging," *Ann. Neurol.*, vol. 26, no. 4, pp. 551–557, 1989.

[18] "Bradykinesia | European Parkinson's Disease Association," *EPDA*, 2017. [Online]. Available:https://www.epda.eu.com/about-parkinsons/symptoms/motor symptoms/bradykinesia/. [Accessed: 03-May-2019].

[19] A. Blochberger and S. Jones, "Parkinson's disease clinical features and diagnosis," *Clin. Pharm.*, vol. 3, no. 11, pp. 361–366, 2011.

[20] "Tremor | European Parkinson's Disease Association," *EPDA*, 2017. [Online]. Available:https://www.epda.eu.com/about-parkinsons/symptoms/motor-symptoms/tremor/. [Accessed: 05-May-2019].

[21] E. Broussolle, P. Krack, S. Thobois, J. Xie-Brustolin, P. Pollak, and C. G. Goetz, "Contribution of Jules Froment to the study of parkinsonian rigidity," *Movement Disorders*, vol. 22, no. 7. pp. 909–914, 2007.

[22] E. Tolosa, G. Wenning, and W. Poewe, "The diagnosis of Parkinson's disease," *Lancet Neurol*, vol. 5, no. 1, pp. 75–86, 2006.

[23] "Progressive Supranuclear Palsy (PSP) | European Parkinson's Disease Association," 2017. [Online]. Available: https://www.epda.eu.com/about-parkinsons/types/progressive-supranuclear-palsy-psp/. [Accessed: 19-May-2019].

[24] "Multiple System Atrophy (MSA) | European Parkinson's Disease Association," 2017. [Online]. Available: https://www.epda.eu.com/about-parkinsons/types/multiple-system-atrophy-msa/. [Accessed: 19-May-2019].

[25] K. D. Seifert and J. I. Wiener, "The impact of DaTscan on the diagnosis and management of movement disorders: A retrospective study," *Am J Neurodegener Dis*, vol. 2, no. 1, pp. 29–34, 2013.

[26] D. Kahraman, C. Eggers, H. Schicha, L. Timmermann, and M. Schmidt, "Visual assessment of dopaminergic degeneration pattern in 123I-FP-CIT SPECT differentiates patients with atypical parkinsonian syndromes and idiopathic Parkinson's disease," *J. Neurol.*, vol. 259, pp. 251–260, 2012.

[27] A. Schrag, Y. Ben-Shlomo, and N. Quinn, "How valid is the clinical diagnosis of Parkinson's disease in the community ?," *J Neurol Neurosurg Psychiatry*, vol. 73, pp. 529–534, 2002.

[28] A. Antonini, P. Berto, S. Lopatriello, F. Tamma, L. Annemans, and M. Chambers, "Cost-Effectiveness of 123 I-FP-CIT SPECT in the Differential Diagnosis of Essential Tremor and Parkinson ' s Disease in Italy," *Mov Disord*, vol. 23, no. 15, pp. 2202–2209, 2008.

[29] "European Parkinson's Disease Association," 2014. [Online]. Available: https://www.epda.eu.com/about-parkinsons/types/dementia-with-lewy-bodies-dlb/. [Accessed: 19-May-2019].

[30] F. Brigo, G. Turri, and M. Tinazzi, "123I-FP-CIT SPECT in the differential diagnosis between Dementia with Lewy bodies and other dementias," *J. Neurol. Sci.*, 2015.

[31] R. Prashanth and S. D. Roy, "Novel and Improved Stage Estimation in Parkinson ' s Disease using Clinical Scales and Machine Learning," *Neurocomputing J.*, vol. 305, p. pp.78-103, 2018.

[32] C. Ramaker, J. Marinus, A. M. Stiggelbout, and B. J. van Hilten, "Systematic evaluation of rating scales for impairment and disability in Parkinson's disease," *Mov. Disord.*, vol. 17, no. 5, pp. 867–876, 2002.

[33] M. Bieńkiewicz and M. Górska-chrząstek, "Impact of CT based attenuation correction on quantitative assessment of DaTSCAN (I-Ioflupane) imaging in diagnosis of extrapyramidal diseases," *Nucl. Med. Rev.*, vol. 11, no. 2, pp. 53–58, 2008.

[34] P. Piccini, A.-A. Roussakis, and M. Politis, "Clinical utility of DaTscan ™ (123I-Ioflupane Injection) in the diagnosis of Parkinsonian Syndromes," *Degener Neurol Neuromuscul Dis.*, vol. 3, pp. 33–39, 2013.

[35] Diagnostic and Interventional Cardiology, "Patient Killed During Nuclear Imaging Scan | DAIC," 2013. [Online]. Available: https://www.dicardiology.com/article/patient-killed-during-nuclear-imaging-scan. [Accessed: 19-May-2019].

[36] GE Healthcare, "SPECT Imaging with DaTscan : How it can help with a parkinsonian syndrome diagnosis.," *General Electric Healthcare.*, 2019. [Online]. Available: http://us.datscan.com/patient/about-datscan/. [Accessed: 26-Apr-2019].

[37] F. N. Emamzadeh and A. Surguchov, "Parkinson's disease: Biomarkers, treatment, and risk factors," *Front. Neurosci.*, vol. 12, no. AUG, pp. 1–14, 2018.

[38] D. J. Brooks, "Imaging dopamine transporters in Parkinsons disease," *Biomark. Med.*, vol. 4, no. 5, pp. 651–660, 2010.

[39] M. Akahoshi *et al.*, "Attenuation and scatter correction in I-123 FP-CIT SPECT do not affect the clinical diagnosis of dopaminergic system neurodegeneration," *Med. (United States)*, vol. 96, no. 45, pp. 1–6, 2017.

[40] F. P. M. Oliveira, D. B. Faria, D. C. Costa, M. Castelo-Branco, and J. M. R. S. Tavares, "Extraction, selection and comparison of features for an effective automated computer-aided diagnosis of Parkinson's disease based on [123 I]FP-CIT SPECT images," *Eur. J. Nucl. Med. Mol. Imaging*, vol. 45, no. 6, pp. 1052–1062, 2018.

[41] G. Cuberas-borro *et al.*, "Quantitative Evaluation of Striatal I-123-FP-CIT Uptake in Essential," *Clin. Nucl. Med.*, vol. 36, no. 11, pp. 991–996, 2011.

[42] L. Wang, Q. Zhang, H. Li, and H. Zhang, "SPECT molecular imaging in Parkinson's disease," *J. Biomed. Biotechnol.*, vol. 2012, p. 11, 2012.

[43] Q. Zhang, L. Li, B. Miao, and H. Niu, "Combining diffusion tensor imaging and susceptibility weighted imaging on the substantia nigra of 1-methyl-4-phenyl-1,2,3,6-tetrahydropyridine (MPTP)-induced rhesus monkey model of Parkinson's disease," *West Indian Med. J.*, vol. 64, no. 5, pp. 480–486, 2015.

[44] S. J. Son, M. Kim, and H. Park, "Imaging analysis of Parkinson's disease patients using SPECT and tractography," *Sci. Rep.*, vol. 6, pp. 1–11, 2016.

[45] H. Murakami *et al.*, "Usefulness Differs Between the Visual Assessment and Specific Binding Ratio of 123I-Ioflupane SPECT in Assessing Clinical Symptoms of Drug-Naïve Parkinson's Disease Patients," *Front. Aging Neurosci.*, vol. 10, no. December, pp. 1–8, 2018.

[46] S. Collado-Vázquez and J. M. Carrillo, "Balzac y el análisis de la marcha humana," *Neurologia*, vol. 30, no. 4, pp. 240–246, 2015.

[47] L. Gastaldi, V. Agostini, R. Takeda, S. Pastorelli, and S. Tadano, "Evaluation of the performances of two wearable systems for gait analysis: A pilot study," *Int. J. Appl. Eng. Res.*, vol. 11, no. 16, pp. 8820–8827, 2016.

[48] Abu-Faraj ZO, Harris GF, Smith PA, Hassani S. Human Gait and Clinical Movement Analysis. In: Wiley Encyclopedia of Electrical and Electronics Engineering, Second Edition, John Wiley & Sons, Inc., New York, USA, pp. 1-34, December 15, 2015.

[49] D. H. Sutherland, "History of Gait Analysis - Part II Kinematics," *Gait Posture*, vol. 16, pp. 159–179, 2002.

[50] D. Ganea, E. Mereuta, and C. Mereuta, "Kinematic Analysis of the Human Gait," *NUCEJ*, vol. 16, no. 1, pp. 208–222, 2013.

[51] H. Gulgin, K. Hall, A. Luzadre, and E. Kayfish, "3D gait analysis with and without an orthopedic walking boot," *Gait Posture*, vol. 59, no. April 2017, pp. 76–82, 2018.

[52] "Gait | European Parkinson's Disease Association," 2017. [Online]. Available: https://www.epda.eu.com/about-parkinsons/symptoms/motor-symptoms/gait/. [Accessed: 09-May-2019].

[53] A. Gaenslen and D. Berg, *Early diagnosis of Parkinson' s Disease.*, vol. 90, no. 10. Elsevier Inc., 2010.

[54] W. Aziz and M. Arif, "Complexity analysis of stride interval time series by threshold dependent symbolic entropy," *Eur J Appl Physiol*, vol. 98, no. 1, pp. 30–40, 2006.

[55] W. Zeng, F. Liu, Q. Wang, Y. Wang, L. Ma, and Y. Zhang, "Parkinson's disease classification using gait analysis via deterministic learning," *Neurosci. Lett.*, vol. 633, pp. 268–278, 2016.

[56] A. Mirelman, P. Bonato, R. Camicioli, T. D. Ellis, N. Giladi, and et al. Hamilton, Jamie L, "Review Gait impairments in Parkinson's disease," *Lancet Glob. Heal.*, vol. 4422, no. 19, pp. 1–12, 2019.

[57] M. Akhtaruzzman, A. A. Shafie, and M. R. Khan, "Gait Analysis: Systems, Technologies, and Importance," *J. Mech. Med. Biol.*, vol. 16, no. 07, p. 1630003, 2016.

[58] A. J. Nelson *et al.*, "The validity of the GaitRite and the Functional Ambulation Performance scoring system in the analysis of Parkinson gait 1," *NeuroRehabilitation*, vol. 17, pp. 255–262, 2002.

[59] J. Rueterbories, E. G. Spaich, B. Larsen, and O. K. Andersen, "Methods for gait event detection and analysis in ambulatory systems," *Med. Eng. Phys.*, vol. 32, no. 6, pp. 545–552, 2010.

[60] H. Geyer, A. Seyfarth, and R. Blickhan, "Compliant leg behaviour explains basic dynamics of walking and running," *Proc. R. Soc. B Biol. Sci.*, vol. 273, no. 1603, pp. 2861–2867, 2006.

[61] U. Trinler and R. Baker, "Estimated landmark calibration of biomechanical models for inverse kinematics," *ELSEVIER*, vol. 0, pp. 1–5, 2017.

[62] A. Salimi-Badr, M. M. Ebadzadeh, and C. Darlot, "A possible correlation between the basal ganglia motor function and the inverse kinematics calculation," *J. Comput. Neurosci.*, vol. 43, no. 3, pp. 295–318, 2017.

[63] E. J. Haug, S. C. Wu, and S. M. Yang, "Dynamics of mechanical systems with Coulomb friction, stiction, impact and constraint addition-deletion-I theory," *Mech. Mach. Theory*, vol. 21, no. 5, pp. 401–406, 1986.

[64] S. Sprager and M. B. Juric, *Inertial sensor-based gait recognition: A review*, vol. 15, no. 9. 2015.

[65] A. Vienne, R. P. Barrois, S. Buffat, D. Ricard, and P. Vidal, "Inertial Sensors to Assess Gait Quality in Patients with Neurological Disorders : A Systematic Review of Technical and Analytical Challenges," vol. 8, no. May, pp. 1–12, 2017.

[66] B. Najafi, K. Aminian, F. Loew, Y. Blanc, and P. Robert, "The measure of stand-sit and sit-stand transition using miniature gyroscope: Falling risk evaluation in elderly," *IEEE Trans. Biomed. Egineering*, vol. 49, no. 8, pp. 843–851, 2002.

[67] M. Al-amri, K. Nicholas, K. Button, L. Sheeran, and J. L. Davies, "Inertial Measurement Units for Clinical Movement Analysis : Reliability and Concurrent Validity," *MDPI*, pp. 1–29, 2018.

[68] Y. S. Suh, "Inertial Sensor-Based Smoother for Gait Analysis," *Sensors*, vol. 14, pp. 24338–24357, 2014.

[69] A. Muro-de-la-Herran, B. García-Zapirain, and A. Méndez-Zorrilla, "Gait analysis methods: An overview of wearable and non-wearable systems, highlighting clinical applications," *Sensors (Switzerland)*, vol. 14, no. 2, pp. 3362–3394, 2014.

[70] D. T. P. Fong and Y. Y. Chan, "The use of wearable inertial motion sensors in human lower limb biomechanics studies: A systematic review," *Sensors (Switzerland)*, vol. 10, no. 12, pp. 11556–11565, 2010.

[71] J. J. Kavanagh and H. B. Menz, "Accelerometry: A technique for quantifying movement patterns during walking," *Gait Posture*, vol. 28, no. 1, pp. 1–15, 2008.

[72] F. Porciuncula *et al.*, "Wearable Movement Sensors for Rehabilitation : A Focused Review of Technological and Clinical Advances," *PM&R*, vol. 10, no. 9, pp. S220–S232, 2018.

[73] A. Rajagopal, C. L. Dembia, M. S. Demers, D. D. Delp, J. L. Hicks, and S. L. Delp, "Full body musculoskeletal model for muscle- driven simulation of human gait," *Trans. Biomed. Eng.*, vol. 63, no. 10, pp. 2068–79, 2016.

[74] M. Miezal, B. Taetz, and G. Bleser, "Real-time inertial lower body kinematics and ground contact estimation at anatomical foot points for agile human locomotion Real-time inertial lower body kinematics and ground contact estimation at anatomical foot points for agile human locomotion," Germany, 48, 2017.

[75] S. Futamure, V. Bonnet, R. Dumas, and G. Venture, "A sensitivity analysis method for the body segment inertial parameters based on ground reaction and joint moment regressor matrices," *J. Biomech.*, 2017.

[76] M. M. Mukaka, "Statistics Corner : A guide to appropriate use of Correlation coefficient in medical research," *Malawi Med. J.*, vol. 24, no. September, pp. 69–71, 2012.

[77] P. S. Corrêa and F. Cechetti, "Is the dopaminergic loss associated with gait and postural impairments in subjects with Parkinson ' s disease at different motor stages ?," *Eur J Neurosci*, no. June, pp. 1–7, 2019.

8 Appendices

8.1 Appendix 1

Table 8.1: List of the equipment used in this dissertation work.

Name	Company
15x MTw Awinda Wireless 3DOF Motion Tracker	Xsens
15x Velcro Full Body Straps Set	
1x Awinda Recording and Docking Station	
1x Awinda Receiving Dongle	
1x MTw Software Development Kit	

8.2 Appendix 2

Table 8.2: List of the software used in this dissertation work.

Name	Company	Version
ITK-SNAP	*https://www.itksnap.org*	3.8.0
Link		
Kinetikos	*https://www.platform.kinetikos.io*	2016-19
Python language		
Excel		
SPSS Statistics		22.0

8.3 Appendix 3

Table 8.3: Mean of clinical characteristics of the striatum.

	Abnormal /With denervation (n = 10)		**Normal /Without denervation (n = 11)**	
	Right (Mean ± Std)	Left (Mean ± Std)	Right (Mean ± Std)	Left (Mean ± Std)
SBR (a.u.)	3.10 ± 0.06	3.01 ± 0.06	4.77 ± 0.15	4.57 ± 0.15
CBP (a.u.)	1.26 ± 0.04	1.28 ± 0.04	2.06 ± 0.16	2.00 ± 0.16
PBP (a.u.)	0.71 ± 0.05	0.67 ± 0.05	1.51 ± 0.15	1.48 ± 0.15
SBP (a.u.)	0.96 ± 0.04	0.95 ± 0.04	1.76 ± 0.15	1.72 ± 0.15
PCR (a.u.)	0.54 ± 0.10	0.54 ± 0.10	0.74 ± 0.11	0.74 ± 0.11
Volume (mm^3)	1.45 ± 0.15	1.15 ± 0.15	7.31 ± 0.58	6.49 ± 0.58
Width (mm)	9.42 ± 0.07	10.24 ± 0.07	20.20 ± 0.19	19.54 ± 0.19
Length (mm)	10.41 ± 0.06	11.59 ± 0.06	33.28 ± 0.22	32.97 ± 0.22
Thickness (mm)	12.55 ± 0.09	12.72 ± 0.09	24.34 ± 0.21	23.28 ± 0.21

Abbreviations:

Uptake ratio features: SBR Specific Binding Ratio, CBP Caudate Binding Potential, PBP Putamen Binding Potential, SBP Striatum Binding Potential, PCR Putamen to Caudate Ratio.

Others: n sample size, Std standard deviation, a.u. arbitrary units.

Data are expressed as mean ± standard deviation.

Table 8.4: Clinical data of the high SBR sides of an abnormal and a normal DAT-Scan

	Abnormal DAT-Scan / Individual with denervation (n = 10)	**Normal DAT-Scan / Individual without denervation (n = 11)**	***p-value***
	(Mean ± Std)	**(Mean ± Std)**	
SBR (a.u.)	3.28. ± 0.94	4.77 ± 1.23	**0.035*[a]**
CBP (a.u.)	1.64 ± 0.27	2.07 ± 0.31	**0.043*[a]**
PBP (a.u.)	0.79 ± 0.26	1.53 ± 0.28	**<0.001*[a]**
SBP (a.u.)	1.18 ± 0.24	1.77 ± 0.29	**0.009*[a]**
PCR (a.u.)	0.54 ± 0.05	0.76 ± 0.07	**<0.001*[a]**
Volume (mm^3)	2848.00 ± 0.35	7759.08 ± 2897.60	**0.001*[a]**
Width (mm)	14.28 ± 0.40	20.58 ± 3.28	**0.035*[a]**
Length (mm)	15.04 ± 0.92	34.08 ± 4.61	**<0.001*[a]**
Thickness (mm)	16.97 ± 0.37	24.81 ± 3.88	**0.009*[a]**

Abbreviations:

Uptake ratio features: SBR Specific Binding Ratio, CBP Caudate Binding Potential, PBP Putamen Binding Potential, SBP Striatum Binding Potential, PCR Putamen to Caudate Ratio.
Others: a.u. arbitrary units, n sample size.
Data are expressed as mean ± standard deviation.

[a=]t test: *High SBR side* of abnormal vs. normal DaTScan (*p* <0.05- *Statistically significant difference).

8.4 Appendix 4

Table 8.5: Mean of bilateral gait metrics.

	Abnormal/ With denervation (n = 10)		**Normal /Without denervation (n = 11)**	
	Right (Mean ± Std)	Left (Mean ± Std)	Right (Mean ± Std)	Left (Mean ± Std)
Cycle duration (s)	1.14 ± 0.10		1.16 ± 0.06	
Support phase dur $(\%)$	67.83 ± 2.67	68.95 ± 2.02	68.52 ± 1.69	66.92 ± 2.60
Swing phase dur $(\%)$	32.17 ± 2.67	31.05 ± 2.02	31.48 ± 1.69	33.08 ± 2.60
Cadence $(steps/min)$	108.29 ± 8.79		104..09 ± 4.54	
Step duration (s)	0.58 ± 0.06	0.55 ± 0.05	0.58 ± 0.04	0.58 ± 0.04
Step duration as $(\%)$	1.78 ± 0.11		1.21 ± 0.90	
Step length (cm)	45.92 ± 7.36	43.87 ± 10.83	48.62 ± 4.22	46.52 ± 5.42
Step length as $(\%)$	3.74 ± 2.49		5.66 ± 3.46	
Step height (cm)	4.31 ± 2.15	4.14 ± 2.51	4.61 ± 1.43	4.66 ± 2.29
Step width (cm)	15.08 ± 3.41		11.91 ± 5.36	
Gait speed (m/s)	0.83 ± 0.23		0.84 ± 0.11	
Double support ph $(\%)$	18.41 ± 2.08		17.01 ± 2.10	
Double support ph1 $(\%)$	18.38 ± 2.91		18.75 ± 2.05	
Arm swing (cm)	37.33 ± 11.93	46.36 ± 21.36	40.85 ± 12.72	43.79 ± 14.54

Abbreviations:

Gait metrics: Support phase dur Support phase duration, Swing phase dur Swing phase duration, Step duration as Step duration asymmetry, Step length as Step length asymmetry, Double support ph Double support phase, Double support ph1 Double support phase 1.

Others: n sample size.

Data are expressed as mean ± standard deviation.

Table 8.6: Kinematics data of the Best side of the body in individuals with and without denervation.

	Individual with denervation (n = 10)	**Individual without denervation (n = 11)**	***p-value***
	(Mean ± Std)	**(Mean ± Std)**	
Support phase dur (%)	69.12 ± 2.67	68.73 ± 1.79	0.385[a]
Swing phase dur (%)	32.34 ± 2.99	33.29 ± 2.44	0.418[a]
Step duration (s)	0.58 ± 0.08	0.59 ± 0.03	0.341[a]
Step length (cm)	44.90 ± 11.17	44.48 ± 4.22	0.260[a]
Step height (cm)	4.23 ± 2.47	3.79 ± 1.79	0.170[a]
Arm swing (cm)	41.93 ± 19.47	46.03 ± 11.79	0.748[a]

Abbreviations:

Kinematics variables: Support phase dur Support phase duration, Swing phase dur Swing phase duration.

Others: n sample size.
Data are expressed as mean ± standard deviation.

[a] =t test: worst side vs. best side of individuals with denervation, (*p* <0.05 - *Statistically significant difference).

8.5 Appendix 5

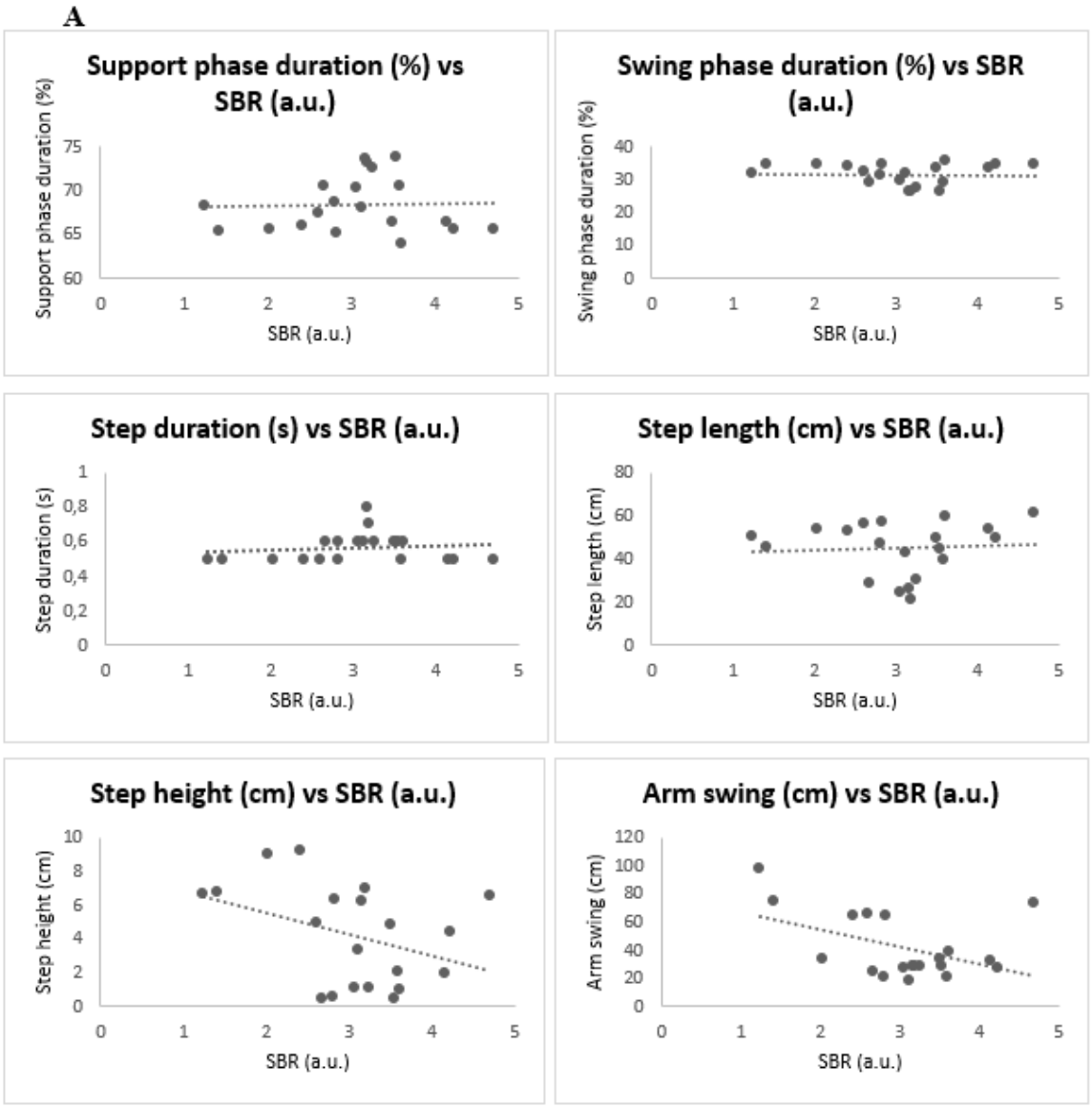

Figure 8.1| A) Scatterplots of correlations of data gathered from the inertial sensors and Specific Binding Ratio - SBR (a.u.) of individuals with denervation. **On left top corner**, Correlation between support phase duration (%) and SBR; **on right top corner**, Correlation between swing phase duration (%) and SBR; **on middle left,** Correlation between step duration (s) and SBR; **on middle right**, Correlation between step length (cm) and SBR; **on left bottom corner**, Correlation between step height (cm) and SBR, and **on right bottom corner,** Correlation between arm swing (cm) and SBR.

B

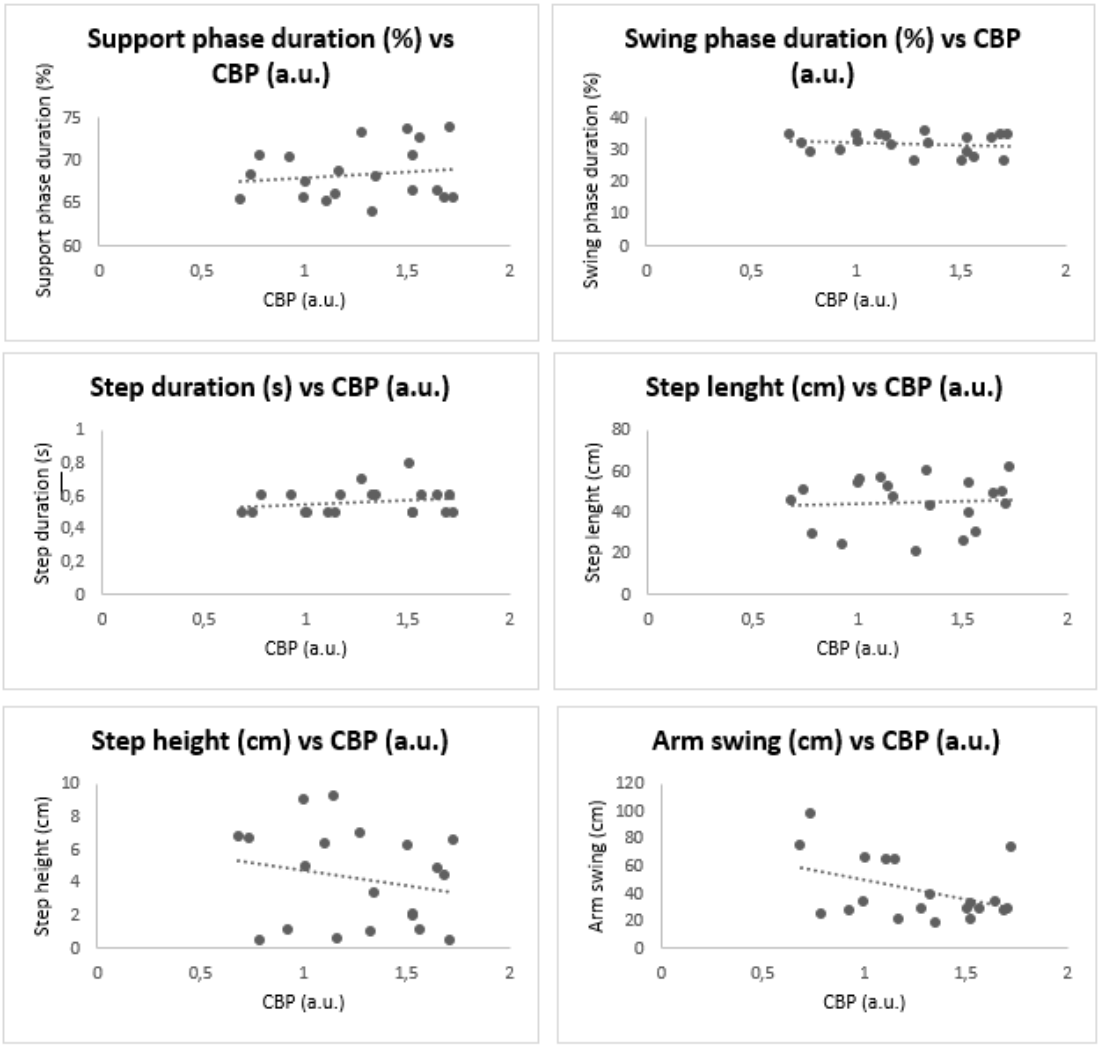

Figure 8.2| B) Scatterplots of correlations of data gathered from the inertial sensors and Caudate Binding Potential - CBP (a.u.) of individuals with denervation. **On left top corner**, Correlation between support phase duration (%) and CBP; **on right top corner**, Correlation between swing phase duration (%) and CBP; **on middle left,** Correlation between step duration (s) and CBP; **on middle right**, Correlation between step length (cm) and CBP; **on left bottom corner**, Correlation between step height (cm) and CBP, and **on right bottom corner,** Correlation between arm swing (cm) and CBP.

C

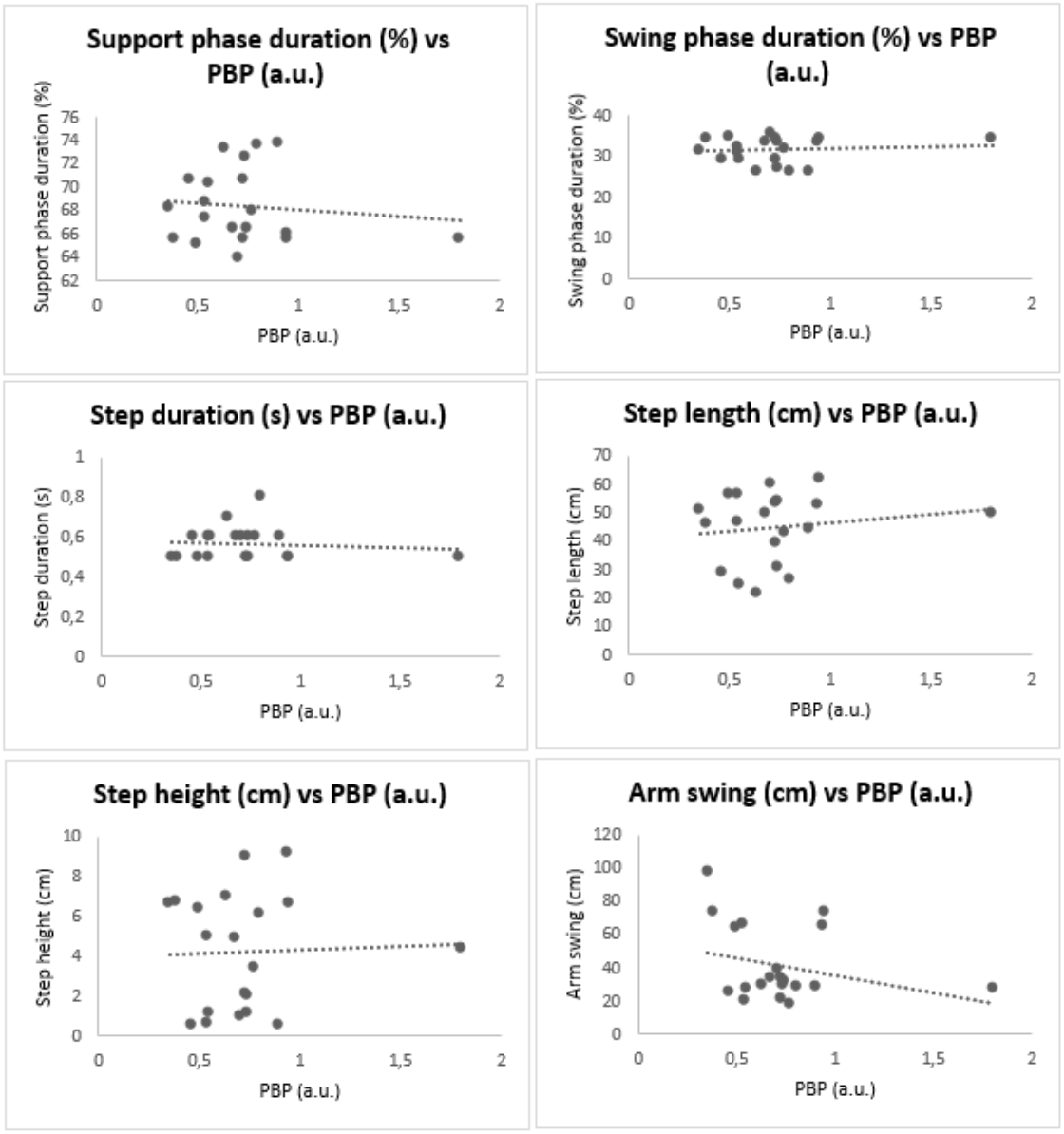

Figure 8.3| C) Scatterplots of correlations of data gathered from the inertial sensors and Putamen Binding Potential - PBP (a.u.) of individuals with denervation. **On left top corner**, Correlation between support phase duration (%) and PBP; **on right top corner**, Correlation between swing phase duration (%) and PBP; **on middle left,** Correlation between step duration (s) and PBP; **on middle right**, Correlation between step length (cm) and PBP; **on left bottom corner**, Correlation between step height (cm) and PBP, and **on right bottom corner,** Correlation between arm swing (cm) and PBP.

D

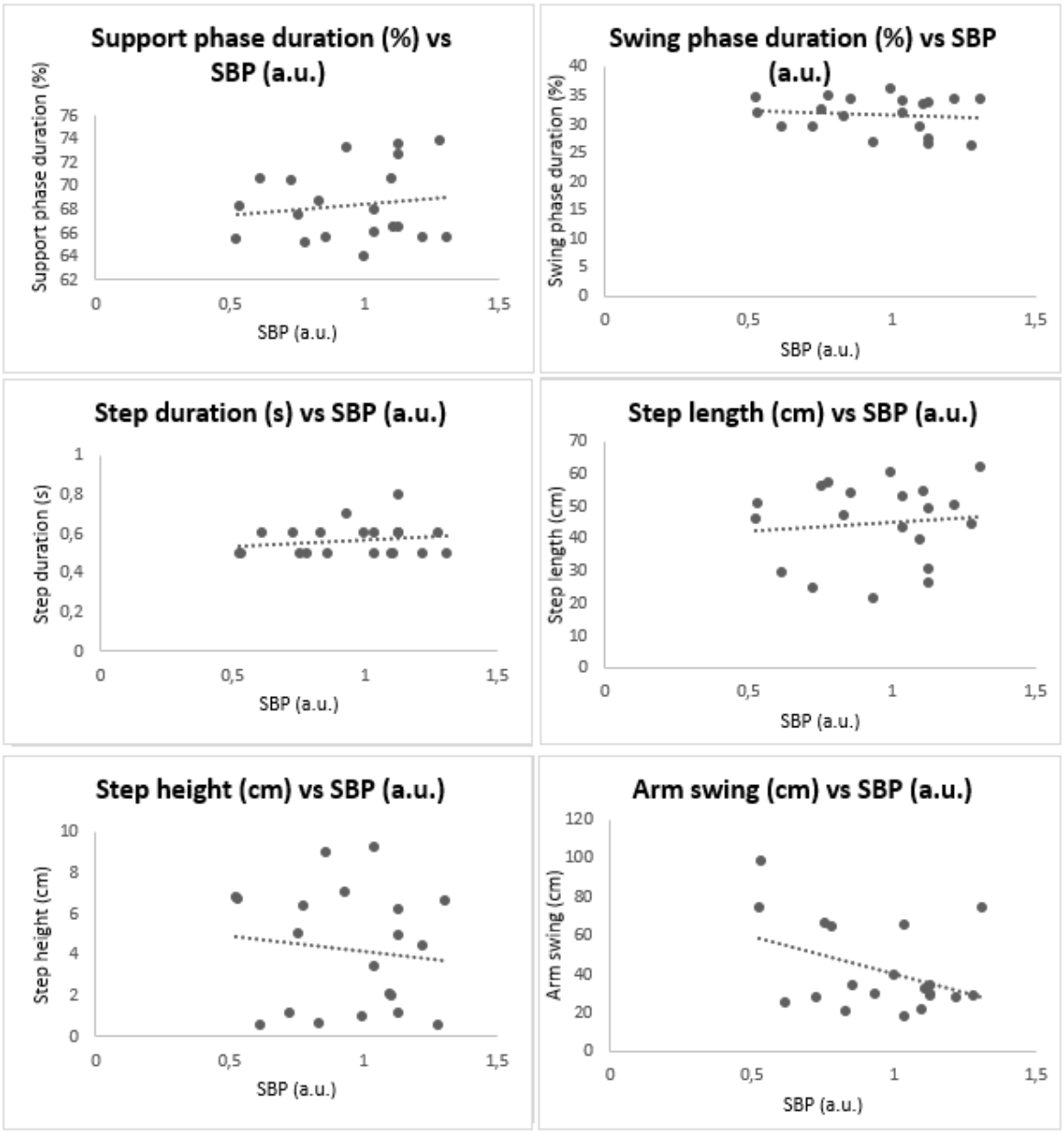

Figure 8.4| D) Scatterplots of correlations of data gathered from the inertial sensors and Striatum Binding Potential - SBP (a.u.) of individuals with denervation. On left top corner, Correlation between support phase duration (%) and SBP; **on right top corner**, Correlation between swing phase duration (%) and SBP; **on middle left,** Correlation between step duration (s) and SBP; **on middle right**, Correlation between step length (cm) and SBP; **on left bottom corner**, Correlation between step height (cm) and SBP, and **on right bottom corner,** Correlation between arm swing (cm) and SBP.

E

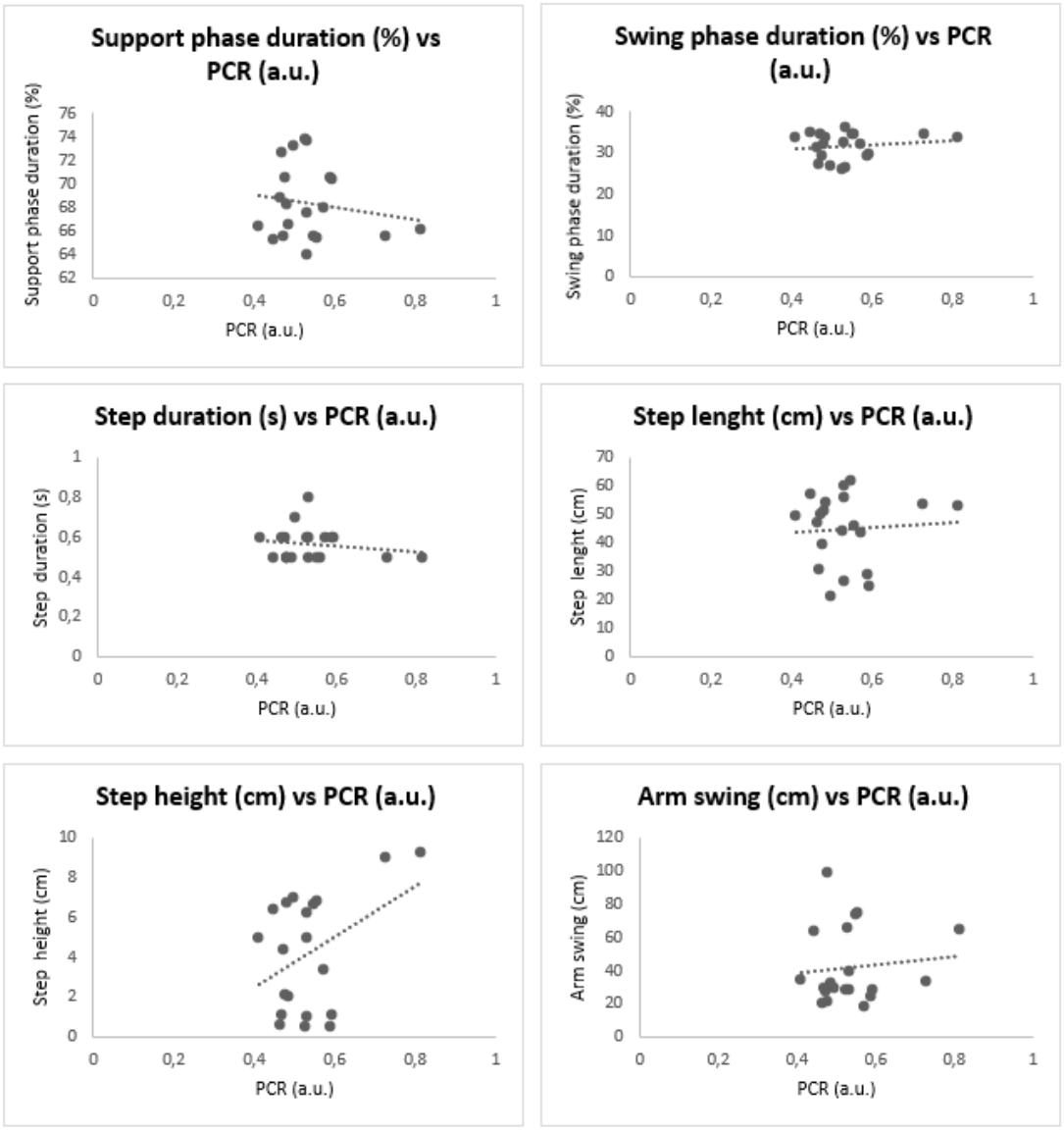

Figure 8.5 | E) Scatterplots of correlations of data gathered from the inertial sensors and Putamen to Caudate Ratio - PCR (a.u.) of individuals with denervation. On left top corner, Correlation between support phase duration (%) and PCR; **on right top corner**, Correlation between swing phase duration (%) and PCR; **on middle left,** Correlation between step duration (s) and PCR; **on middle right**, Correlation between step length (cm) and PCR; **on left bottom corner**, Correlation between step height (cm) and PCR, and **on right bottom corner,** Correlation between arm swing (cm) and PCR.

F

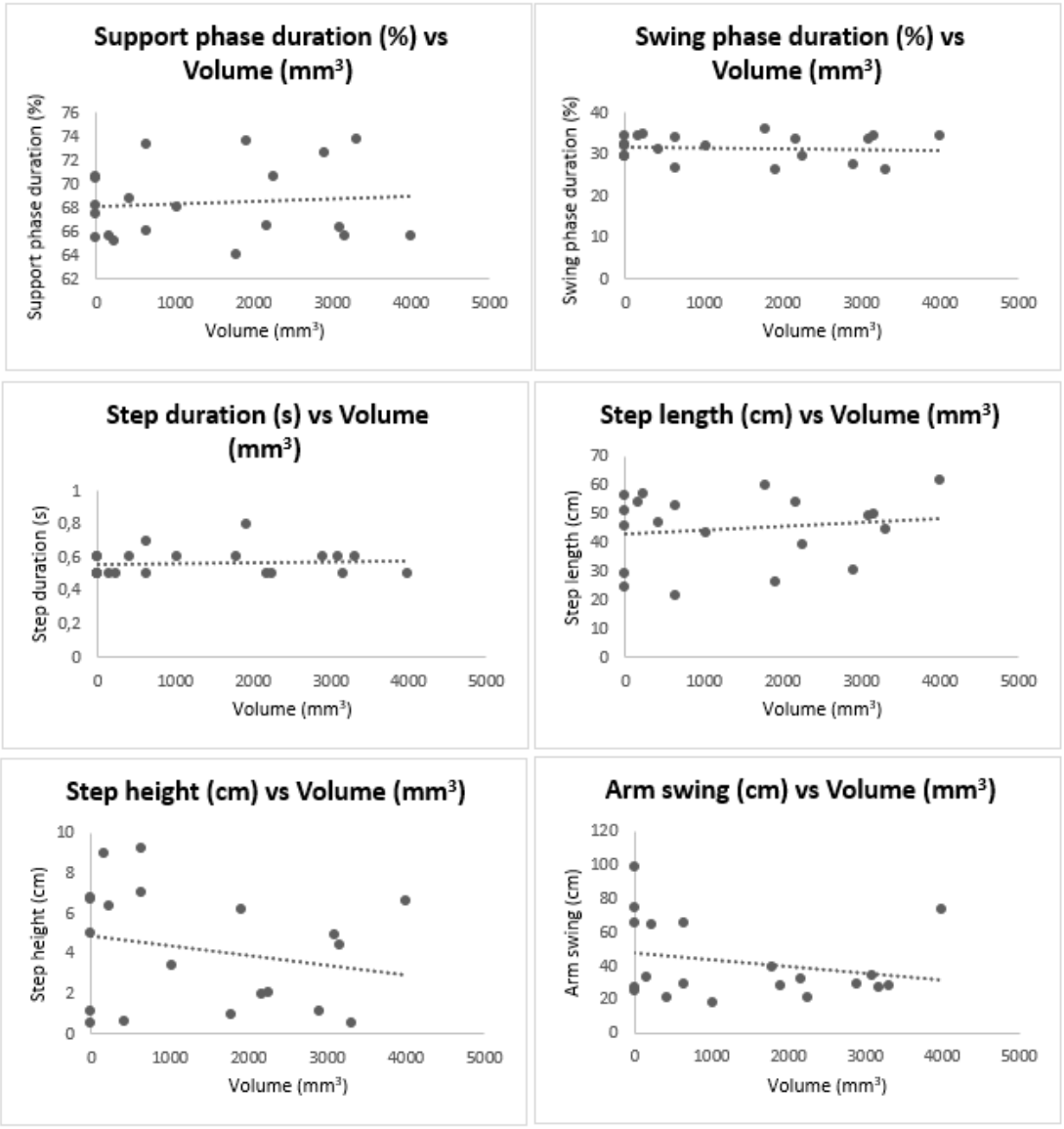

Figure 8.6| F) Scatterplots of correlations of data gathered from the inertial sensors and volume (mm³) of individuals with denervation. On left top corner, Correlation between support phase duration (%) and volume; **on right top corner**, Correlation between swing phase duration (%) and volume; **on middle left,** Correlation between step duration (s) and volume; **on middle right**, Correlation between step length (cm) and volume; **on left bottom corner**, Correlation between step height (cm) and volume, and **on right bottom corner,** Correlation between arm swing (cm) and volume.

G

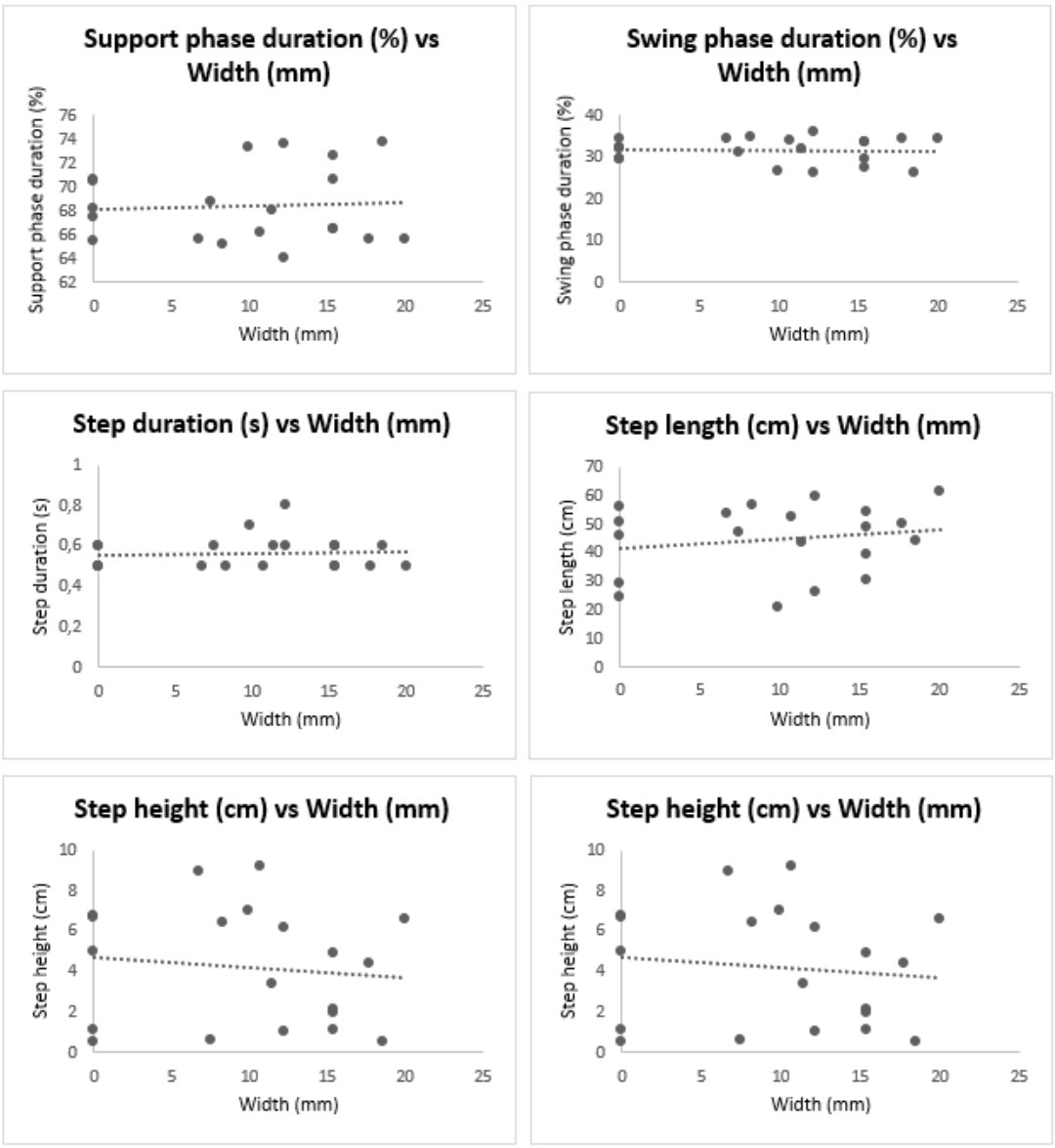

Figure 8.7| G) Scatterplots of correlations of data gathered from the inertial sensors and width (mm) of individuals with denervation: On left top corner, Correlation between support phase duration (%) and width; **on right top corner**, Correlation between swing phase duration (%) and width; **on middle left,** Correlation between step duration (s) and width; **on middle right**, Correlation between step length (cm) and width; **on left bottom corner**, Correlation between step height (cm) and width, and **on right bottom corner,** Correlation between arm swing (cm) and width.

H

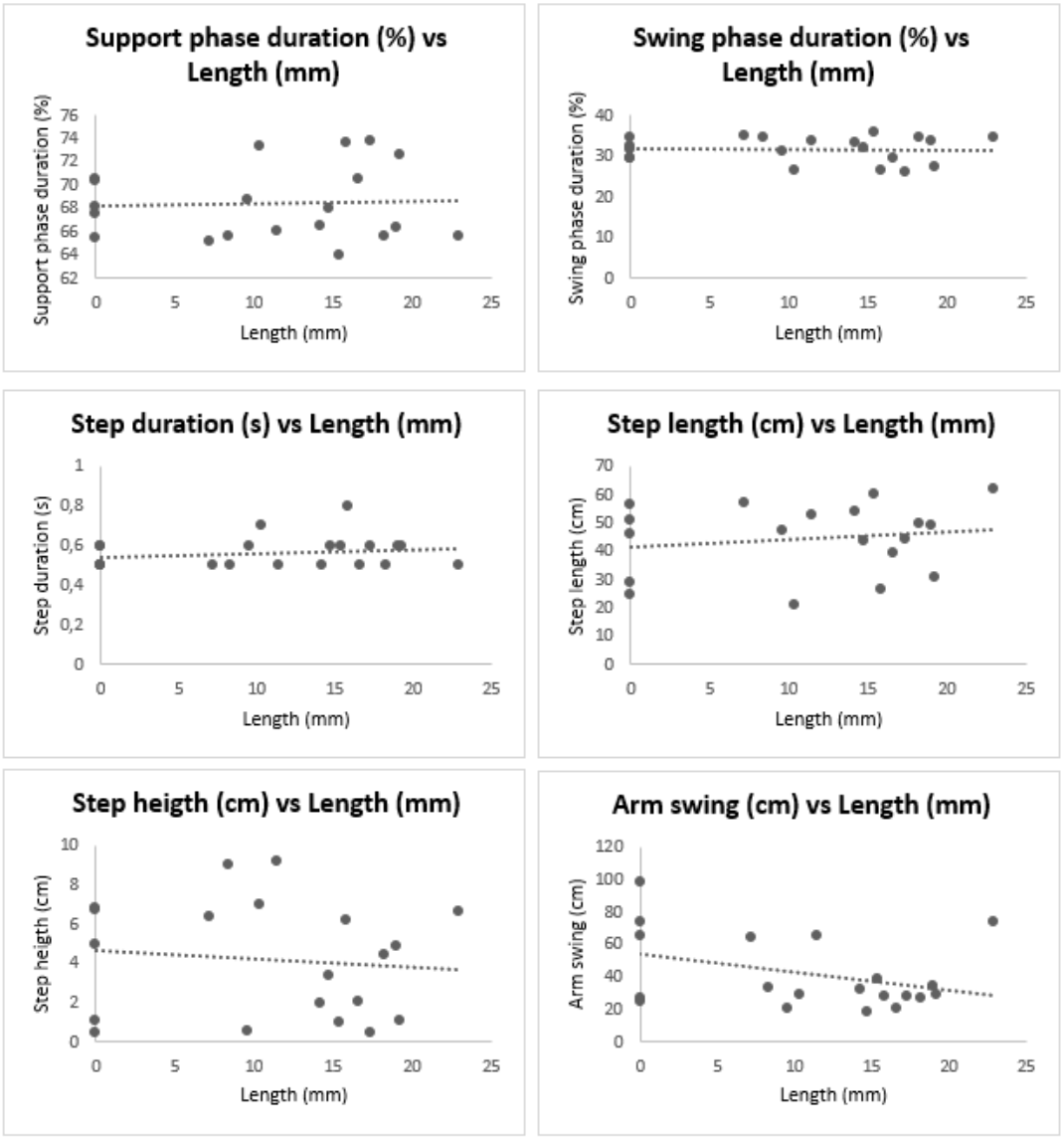

Figure 8.8| H) Scatterplots of correlations of data gathered from the inertial sensors and length (mm) of individuals with denervation: On left top corner, Correlation between support phase duration (%) and length; **on right top corner**, Correlation between swing phase duration (%) and length; **on middle left,** Correlation between step duration (s) and length; **on middle right**, Correlation between step length (cm) and length; **on left bottom corner**, Correlation between step height (cm) and length, and **on right bottom corner,** Correlation between arm swing (cm) and length.

I

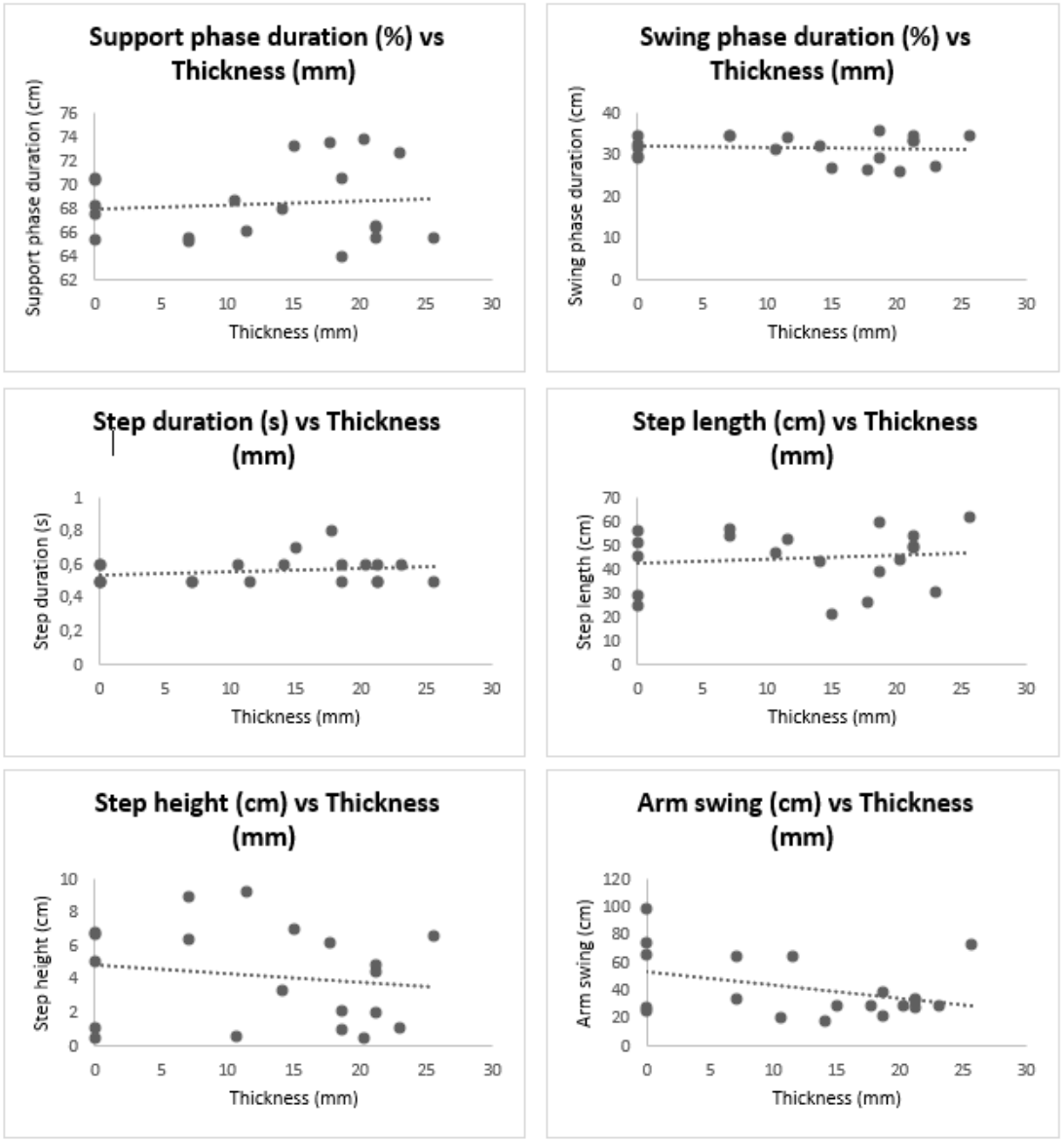

Figure 8.9 | I) Scatterplots of correlations of data gathered from the inertial sensors and thickness (mm) of individuals with denervation: On left top corner, Correlation between support phase duration (%) and thickness; **on right top corner**, Correlation between swing phase duration (%) and thickness; **on middle left,** Correlation between step duration (s) and thickness; **on middle right**, Correlation between step length (cm) and thickness; **on left bottom corner**, Correlation between step height (cm) and thickness, and **on right bottom corner,** Correlation between arm swing (cm) and thickness.